

An Algorithm for the Construction of Global Reduced Mechanisms With CSP Data

A. MASSIAS,[†] D. DIAMANTIS,[‡] E. MASTORAKOS, and D.A. GOUSSIS*

Institute of Chemical Engineering and High Temperature Processes, ICEHT-FORTH, 26500 Rio-Patra, Greece

[†]Mechanical and Aerospace Engineering Department, University of Patras,

26500 Rio-Patra, Greece, [‡]Chemical Engineering Department, University of Patras,

26500 Rio-Patra, Greece

An algorithm is presented for the construction of global reduced mechanisms, based on concepts from the Computational Singular Perturbation method. Input to the algorithm are (i) the detailed mechanism, (ii) a representative numerical solution of the problem under investigation, and (iii) the desired number of steps in the reduced mechanism. The algorithm numerically identifies the “steady-state” species and fast reactions and constructs the reduced mechanism. The stoichiometric coefficients are constant and are connected to the non “steady-state” species, while the related rates involve the slow elementary rates only. The proposed method is applied to a laminar premixed CH₄/Air flame and a complex detailed chemical kinetics mechanism, consisting of 279 reactions and 49 species and accounting for both thermal and prompt NO_x production. A seven-step mechanism is constructed which is shown to reproduce the species profiles and the laminar burning velocity very accurately over a wide range of values for the initial mixture composition and temperature. In addition, it is shown that the seven-step mechanism introduces much lower time scales than the detailed mechanism does. Since the proposed procedure for constructing reduced mechanisms is fully algorithmic and requires minor computations, it is very much suited for the simplification of large detailed mechanisms. © 1999 by The Combustion Institute

INTRODUCTION

The simulation of combustion processes is aiming at the numerical prediction of the most important physical variables (e.g., velocities, species mass fractions, etc.) for given operating conditions and the identification of the most important physical processes (e.g., rate controlling reactions, etc.) in the problem under study. The numerical solution of the governing equations faces two major obstacles. The first problem is due to the stiffness introduced by the fast time scales due to the kinetics term in the species governing equations. The second problem is created by the large number of unknowns resulting after the discretization of the governing equations, becoming more serious when large detailed chemical kinetic mechanisms are used. Both these problems (stiffness and large systems of equations) make the simulation of even relatively simple flames (i.e., laminar 2D) a tedious and time-consuming effort [1]. The identification of the most significant physical parameters in the process is important for the physical understanding of the problem and the

design and specification of operating conditions in combustion devices (i.e., increased efficiency, reduction of pollutants, etc.). Usually, such identifications are based on sensitivity analysis [2]. However, when complex detailed kinetics mechanisms are employed in combustion problems, the large number of unknowns and elementary reactions make the sensitivity analysis a not very efficient tool [3].

These issues are currently faced with the use of reduced mechanisms, for the construction of which a serious effort is underway. Reduced mechanisms consist of a few steps, which involve only a small number of chemical species and the corresponding rates are linear relations among the elementary rates. In comparison to the detailed mechanism, a successful reduced mechanism is free of the fastest time scales and can reproduce the most essential features of the problem under investigation. The most familiar type of reduced mechanisms is that in which the number of steps is fixed and the stoichiometric coefficients and the coefficients multiplying the elementary rates in the expressions of the rates are all constant. Such mechanisms already exist for a number of fuel and flame types [4–7], providing results of high accuracy. Since these mechanisms are valid

*Corresponding author; E-mail: dagoussi@iceht.forth.gr

throughout the computational domain, they are of *global* character. A more recent kind of reduced mechanisms consists of varying with time or space stoichiometric coefficients, coefficients in the expressions of the rates, and possibly number of steps. As a result, these mechanisms can be characterized as *local*. Such mechanisms are constructed with the methods of Computational Singular Perturbation [8–12], Intrinsic Low-Dimensional Manifold [13–17] and Invariant Manifolds [18, 19]. The local mechanisms are more accurate than the global ones [20, 21]. However, this accuracy is obtained at the expense of a higher amount of computations. In the case where efficiency is more desirable than accuracy, global mechanisms must be used.

Given a detailed mechanism, the construction of global reduced mechanisms is based on the introduction of a number of steady state and/or partial equilibrium approximations [22]. Such approximations are valid when the fast chemistry time scales become exhausted. When only steady state approximations are used, it is always possible to construct a global reduced mechanism in which only a small number of species appear in the stoichiometry of its steps. However, this is not always true when partial equilibrium approximations are also involved [20]. In any case, when a reduced mechanism is available, the mass fraction of the species appearing in the stoichiometry of the global mechanism (major species) are computed from the appropriate conservation differential equations while those of the remaining species (minor or “steady-state” species), which are needed for the calculation of the global rates, are computed from the steady state or partial equilibrium relations.

The conventional method for constructing a reduced global mechanism starts with the specification of a detailed mechanism, the operating conditions (e.g., type of flame, initial mixture composition, initial temperature, etc.) and the desired number of steps in the reduced mechanism. The next step relates to the identification of the “steady-state” species and the fast reactions [4, 5]. If the detailed mechanism involves N species and E elements and the global mechanism is desired to consist of S steps, then M “steady-state” species and M fast elementary reactions must be identified, where $M = N - E - S$. On the basis of this information,

reduced mechanisms can be constructed with a numerical algorithm involving simple linear algebra operations [20, 23, 24]. The final step in the construction of reduced mechanisms consists of the simplification (truncation) of the expressions for the steady-state or partial equilibrium relations and global rates, so that the reduced mechanism results in faster computations [4, 5] and more accurate results [26, 27].

Having available a detailed mechanism and a set of operating conditions, the key steps in the procedure described above for constructing global mechanism are (i) the specification of the number of global steps, (ii) the identification of the “steady state” species and the fast elementary reactions, and (iii) the truncation. As discussed in the following, the successful execution of these three steps faces significant obstacles.

When constructing a global reduced mechanism, the goal is to achieve acceptable accuracy with the minimum number of steps S . So far, there is no method to a priori determine this number. In general, S is determined on a trial and error basis or in connection with the number of species which are deemed as reliable candidates to be identified as “steady state.”

Usually, the “steady-state” species are selected as those whose net production rates are much smaller than the sum of production and destruction rates. The mass fraction, or appropriately weighted mass fraction, of these species is sufficiently smaller than those of the remaining ones throughout the computational domain [4, 5, 25]. Such a selection is based on sensible physical grounds for the following reasons. The detailed mechanism introduces a number of fast time scales, which force the trajectory to move on a low dimensional manifold. Any perturbation off the manifold will quickly decay due to the fast physical processes generating the fast time scales. Such fast processes are some elementary reactions in the detailed mechanism which, due to the contracting character of the fast time scales, are related to the fast depletion of certain species. Therefore, the fastest time scales in the problem are related to elementary steps which tend to deplete the fastest certain species. As a result, these particular species never attain large mass fractions. They are characterized as “steady state” since any tendency to increase their mass fraction is quickly

balanced by the fastest elementary steps, resulting in relatively small net production rates. However, such a method for the identification of the “steady-state” species (i.e., low magnitude of the net vs production/destruction rates or small mass fraction) is not always correct, since it is based on the assumption that the mass fraction of all species is of the same magnitude and evolve with the same time scale. This is not always true and wrong conclusions may be obtained.

As fast elementary steps are selected, those which exhibit large depletion rates for the “steady state” species [4, 5, 25] or, equivalently, the most sensitive steps involving those species. From the discussion above it seems that such a selection is correct, on the condition that the “steady state” species were properly identified.

The simplification (truncation) of the expressions for the steady-state or partial equilibrium relations and global rates has two objectives. It aims at (i) the speed-up of the computations and possibly (ii) the correction of the errors produced from the application of the steady-state or partial equilibrium assumptions in the construction of the reduced mechanism. Given that the “steady-state” species and fast elementary reactions were properly identified, for the first objective, it suffices to neglect the elementary rates that contribute little to the cancellations occurring in the steady-state or partial equilibrium relations and to the expressions for the global rates. As for the second objective, the most important tool is sensitivity analysis [2, 26, 27]. Such an analysis requires heavy computations, the results of which are not always conclusive and need further analysis for interpretation [28–30].

From the discussion above, it is clear that the most important decisions that must be taken for the construction of a global reduced mechanism relate to the selection of the number of steps in the mechanism and the identification of the “steady-state” species. For a successful decision on these two questions a robust algorithm does not currently exist. The execution of the steps which follow, i.e. the selection of the fast elementary reactions and the truncation (aiming at the speed-up of computations), does not pose significant problems.

Here, an algorithmic procedure shall be presented for the construction of global reduced

mechanisms on the basis of steady state assumptions. It will be shown how a good estimate on the number of steps in the mechanism can be obtained and how the “steady-state” species can be identified by data generated from the CSP method. The algorithm also includes the identification of the fast elementary reactions, the generation of the reduced mechanism and the truncation of the steady-state relations and the expressions for the global rates. This algorithm will be applied for the construction of a seven-step mechanism from a detailed one consisting of 279 reactions (mostly reversible) and 49 species for the case of CH_4/Air combustion accounting for thermal and prompt NO_x formation. This problem has been the subject of a thorough examination and several global reduced mechanisms have already been developed [4–7, 31–33].

The structure of the manuscript is as follows. First, a brief outline of the CSP method as applied to stiff PDEs shall be presented. Then, a variation of the method shall be developed that can be used for the construction of global reduced mechanisms; the reader who is only interested in the use of the method can ignore this section. The new methodology shall then be applied to a CH_4/Air laminar premixed flame for the construction of a seven-step global mechanism. The range of validity of this mechanism will be examined by comparing numerical results thus obtained with those obtained on the basis of the detailed mechanism for a wide range of operating conditions. Finally, some comments are presented on the possible use of the reduced mechanisms thus obtained in laminar and turbulent combustion simulations.

OUTLINE OF THE CSP METHOD

The Computational Singular Perturbation (CSP) method [8–10] was first developed for the solution and analysis of stiff ODEs and later extended for the treatment of stiff PDEs when the stiffness is produced by a source term [12]. So far the method has been applied to a number of combustion problems involving stirred reactors [34], laminar flames [3, 21, 35–38], and shock induced combustion [39, 40]. Here an overview of the method will be presented in

order to point out the parts of the method that are incorporated in the algorithm for the construction of global reduced mechanisms.

The general form of the species conservation equation is

$$\frac{\partial \mathbf{y}}{\partial t} = \mathbf{L}(\mathbf{y}) + \mathbf{g}(\mathbf{y}), \quad (1a)$$

$$= \mathbf{L}(\mathbf{y}) + \mathbf{W}[\mathbf{S}_1 R^1(\mathbf{y}) + \mathbf{S}_2 R^2(\mathbf{y}) + \dots + \mathbf{S}_K R^K(\mathbf{y})], \quad (1b)$$

$$= \mathbf{L}(\mathbf{y}) + \mathbf{WSR}(\mathbf{y}), \quad (1c)$$

where \mathbf{y} is the N -dimensional vector of species mass fraction, \mathbf{L} is a spatial differential operator (convection – diffusion), and g is a nonlinear function representing the chemical kinetics. \mathbf{W} is a $N \times N$ diagonal matrix with the species molecular weights divided by the total mass density as entries. As it is indicated by Eq. (1b), it is assumed that the detailed chemical kinetics mechanism involves N species and K elementary steps, which are represented by the stoichiometric vectors \mathbf{S}_i and the reaction rates R^i . It is also assumed that the N species are formed by E elements. In Eq. (1c) the columns of the $N \times K$ matrix \mathbf{S} are the K stoichiometric vectors \mathbf{S}_i and the K components of the vector \mathbf{R} are the K elementary rates R^i . At each point in time and space the CSP method provides two sets of N -dimensional column basis vectors \mathbf{a}_i , which define the fast and slow subdomains of \mathbf{y} :

$$\begin{aligned} \mathbf{a}_r &= [\mathbf{a}_1, \mathbf{a}_2, \dots, \mathbf{a}_M] \quad \mathbf{a}_s \\ &= [\mathbf{a}_{M+1}, \mathbf{a}_{M+2}, \dots, \mathbf{a}_N], \end{aligned} \quad (2)$$

where M is the number of time scales, which are faster than the locally dominant ones and varies from 0 to $N - 1$ [8–12]. On the basis of these vectors, Eq. (1) can be cast in the form:

$$\frac{\partial \mathbf{y}}{\partial t} = \mathbf{a}_r \mathbf{h}^r + \mathbf{a}_s \mathbf{h}^s, \quad (3)$$

where

$$\mathbf{h}^r = \mathbf{b}^r(\mathbf{L} + \mathbf{g}) \quad \mathbf{h}^s = \mathbf{b}^s(\mathbf{L} + \mathbf{g}), \quad (4)$$

and the N row vectors in \mathbf{b}^r and \mathbf{b}^s form the dual basis. These vectors are produced by the relations:

$$\mathbf{a}_r = \mathbf{J} \mathbf{a}_{or} \boldsymbol{\tau}_{or}^{\text{or}} \quad \mathbf{b}^s = \mathbf{b}^{\text{os}}[\mathbf{I} - \mathbf{a}_r \mathbf{b}^{\text{or}}], \quad (5a, b)$$

$$\mathbf{b}^r = \boldsymbol{\tau}_r^{\text{or}} \mathbf{b}^{\text{or}} \mathbf{J} \quad \mathbf{a}_s = [\mathbf{I} - \mathbf{a}_r \mathbf{b}^r] \mathbf{a}_{os}, \quad (5c, d)$$

where

$$\boldsymbol{\tau}_{or}^{\text{or}} = (\mathbf{b}^{\text{or}} \mathbf{J} \mathbf{a}_{or})^{-1} \quad \boldsymbol{\tau}_r^{\text{or}} = (\mathbf{b}^{\text{or}} \mathbf{J} \mathbf{a}_r)^{-1}.$$

\mathbf{J} is the Jacobian of the source term \mathbf{g} and the vectors in \mathbf{a}_{or} and \mathbf{a}_{os} (and the dual basis \mathbf{b}^{or} and \mathbf{b}^{os}) are a suitably chosen initial guess [8, 9, 20]. Note that if the right and left eigenvectors of \mathbf{J} are selected for the vectors in $(\mathbf{a}_{or}, \mathbf{a}_{os})$ and $\mathbf{b}^{\text{or}}, \mathbf{b}^{\text{os}}$, respectively, the vectors in $(\mathbf{a}_r, \mathbf{a}_s)$ and $\mathbf{b}^r, \mathbf{b}^s$ are also the right and left eigenvectors of \mathbf{J} . The CSP produced basis vectors guarantee that the M fast amplitudes in \mathbf{h}^r are negligible, i.e.,

$$h^i = \mathbf{b}^i \cdot (\mathbf{L} + \mathbf{g}) \approx 0 \quad i = 1, M \quad (6)$$

The scalar M is determined by the number of amplitudes h^i , which satisfy the inequality

$$|\mathbf{a}_r \mathbf{h}^r| \Delta t_{M+1} < c_1 |\mathbf{y}| + \mathbf{y}_{\text{cut}}, \quad (7)$$

where “ $|\cdot|$ ” denotes the absolute value of the elements in a vector, Δt_{M+1} is a fraction of the time scale related to the $(M + 1)$ -th amplitude, c_1 is a positive number less than one (e.g., 10^{-2} , 10^{-3} , etc.), and \mathbf{y}_{cut} is a vector whose elements are positive and much smaller in absolute value than those in \mathbf{y} .

When the stiffness of Eq. (1) is due to the source term \mathbf{g} , the term $\mathbf{b}^i \cdot \mathbf{L}$ does not contribute much to the cancelations occurring in Eqs. (6) [12]. Therefore, Eqs. (6) can be simplified as

$$\begin{aligned} h^i &\approx (\mathbf{b}^i \cdot \mathbf{WS}_1) R^1 + (\mathbf{b}^i \cdot \mathbf{WS}_2) R^2 \\ &+ \dots + (\mathbf{b}^i \cdot \mathbf{WS}_K) R^K \approx 0, \end{aligned} \quad (8)$$

where $i = 1, M$. Equations (8) are equivalent to the conventional “steady-state” relations and form a manifold on which the trajectory moves. Since the term $\mathbf{a}_r \mathbf{h}^r$ in Eq. (3) is insignificant, the trajectory moves on the manifold with the slow time scales according to the equation:

$$\frac{\partial \mathbf{y}}{\partial t} \approx \mathbf{a}_s \mathbf{h}^s. \quad (9)$$

Note that in the case where eigenvectors are used in Eqs. (5a–d), the simplified form of equations employed by the ILDM method are recovered from Eqs. (9) [13–15]. Expanding the RHS of Eq. (9) yields

$$\frac{\partial \mathbf{y}}{\partial t} \approx \mathbf{a}_s \mathbf{b}^s \mathbf{L} + \mathbf{a}_s \mathbf{b}^s \mathbf{g}. \quad (10)$$

Equation (10) can be further simplified by taking into account the fact that the set of $N - M$ vectors in \mathbf{a}_s and \mathbf{b}^s contain E constant vectors which express the conservation of elements in the elementary reactions. By defining the set of vectors

$$\mathbf{a}_s = [\hat{\mathbf{a}}_s, \mathbf{a}_c] \quad \mathbf{b}^s = [\hat{\mathbf{b}}^s, \mathbf{b}^c]^T \quad (11)$$

where the E vectors in \mathbf{a}_c and \mathbf{b}^c account for the conservation of elements, the simplified system of Eq. (10) simplifies further to

$$\frac{\partial \mathbf{y}}{\partial t} \approx \mathbf{a}_s \mathbf{b}^s \mathbf{L} + \hat{\mathbf{a}}_s \hat{\mathbf{b}}^s \mathbf{g}. \quad (12)$$

It is seen that Eq. (12) involves a simplified spatial operator and a simplified source term. In particular, the $N - M - E$ vectors in $\hat{\mathbf{a}}_s$ are the stoichiometric vectors of the reduced mechanism and the $N - M - E$ scalars in $\hat{\mathbf{b}}^s \mathbf{g}$ are the corresponding rates. Since the basis vectors and the scalar M are explicit functions of \mathbf{y} , the specific size (number of steps) and form of the reduced mechanism in Eq. (12) are functions of time and space.

Given the M algebraic relations (8) and the N differential Eqs. (12), there are two methods to obtain an approximate solution to the original Eq. (1). The first method is to compute all N components of \mathbf{y} from Eq. (12). In that case the homogeneous correction [10, 11]:

$$\mathbf{y} \leftarrow \mathbf{y} - \mathbf{a}_r \tau_r^T (\mathbf{b}^r \mathbf{g}) \quad (13)$$

must be applied at each spatial grid point at the start of a new time step. The correction (13) accounts for the fast time scales ignored in Eq. (12) and keeps the trajectory on the manifold specified by the algebraic relations (8). The second method for obtaining an approximate solution to the full problem is to use the M algebraic relations (8) for the calculation of M elements of \mathbf{y} and $N - M$ components of the differential Eqs. (12) for the remaining ones. The choice on which elements of \mathbf{y} can be computed from the algebraic relations cannot be arbitrary. Stability and accuracy reasons require that these relations must be used for the computation of the M elements of \mathbf{y} whose axes

are the most perpendicular to the manifold and the elementary rates in which they participate have a significant contribution in the cancellations occurring in Eq. (8). The elements whose axis is the most perpendicular to the manifold are identified by the "CSP-pointer," i.e. the diagonal components of the $N \times N$ matrix:

$$[\mathbf{a}_1 \mathbf{b}^1 + \mathbf{a}_2 \mathbf{b}^2 + \dots + \mathbf{a}_M \mathbf{b}^M], \quad (14)$$

which sum up to M [9, 10]. In particular, the M diagonal components with the largest components correspond to the elements of \mathbf{y} the axes which are the most perpendicular to the manifold. Since the fast time scales act along these directions, it follows that the elements of \mathbf{y} which are the most affected by the fast scales are those identified by the "CSP-pointer."

The splitting of the source term \mathbf{g} into a fast ($\mathbf{a}_r \mathbf{b}^r \mathbf{g}$) and a slow ($\hat{\mathbf{a}}_s \hat{\mathbf{b}}^s \mathbf{g}$) component, permits the simplification of the algebraic relations (8) and the expressions of the rates $\hat{\mathbf{b}}^s \mathbf{g}$, as follows. By defining the Participation and Importance Indices [10, 11] as

$$P_j^m = \frac{\mathbf{b}^m \mathbf{W} \mathbf{S}_j R^j}{|\mathbf{b}^m \mathbf{W} \mathbf{S}_1 R^1| + \dots + |\mathbf{b}^m \mathbf{W} \mathbf{S}_K R^K|}, \quad m = 1, M \quad j = 1, K \quad (15)$$

$$I_j^n = \frac{\mathbf{A}^n \mathbf{S}_j R^j}{|\mathbf{A}^n \mathbf{S}_1 R^1| + \dots + |\mathbf{A}^n \mathbf{S}_K R^K|}, \quad n = 1, N \quad j = 1, K \quad (16)$$

where \mathbf{A}^n is the n th row of the N -dimensional matrix $\mathbf{A} = \hat{\mathbf{a}}_s \hat{\mathbf{b}}^s \mathbf{W}$, we can estimate (i) the participation of each elementary step in the cancellations occurring in Eq. (8), which define the manifold and (ii) the importance of each elementary step in the motion of the trajectory on the slow manifold according to Eqs. (10). Since by definition,

$$|P_1^m| + |P_2^m| + \dots + |P_R^m| = 1$$

$$|I_1^n| + |I_2^n| + \dots + |I_R^n| = 1 \quad (17)$$

elementary reactions that produce indices $|P_i^m|$ and $|I_i^n|$ with negligible values can be neglected from the algebraic relations (8) and in the rates of the reduced mechanism in Eq. (10), respectively. The ones that produce significant values are retained.

CONSTRUCTION OF GLOBAL REDUCED MECHANISMS

Since the scalar M and the CSP vectors \mathbf{a}_i and \mathbf{b}^i are \mathbf{y} -dependent, the size and form of the $N - M - E$ step mechanism in Eqs. (12) are also \mathbf{y} -dependent. This is the feature which distinguishes the local reduced mechanisms constructed with the CSP method from the global ones which involve constant \mathbf{a}_i and \mathbf{b}^i vectors [8, 20]. Although they will result in reduced accuracy [20, 21], it is obvious that the availability of constant vectors \mathbf{a}_i and \mathbf{b}^i will speed-up the numerical calculations.

The construction of global reduced mechanisms on the basis of steady state or partial equilibrium approximations is equivalent to the definition of three sets of linearly independent constant N -dimensional column basis vectors \mathbf{a}_i :

$$\begin{aligned}\mathbf{a}_r &= [\mathbf{a}_1, \dots, \mathbf{a}_M] & \mathbf{a}_s &= [\mathbf{a}_{M+1}, \dots, \mathbf{a}_{N-E}] \\ \mathbf{a}_c &= [\mathbf{a}_{N-E+1}, \dots, \mathbf{a}_N]\end{aligned}\quad (18)$$

where N , is the number of species in the detailed kinetics mechanism, E is the number of elements, and M is the number of approximations introduced. These sets of vectors are accompanied by their dual set of constant N -dimensional row vectors \mathbf{b}^i :

$$\mathbf{b}^r = \begin{bmatrix} \mathbf{b}^1 \\ \vdots \\ \mathbf{b}^M \end{bmatrix} \quad \mathbf{b}^s = \begin{bmatrix} \mathbf{b}^{M+1} \\ \vdots \\ \mathbf{b}^{N-E} \end{bmatrix} \quad \mathbf{b}^c = \begin{bmatrix} \mathbf{b}^{N-E+1} \\ \vdots \\ \mathbf{b}^N \end{bmatrix} \quad (19)$$

By expanding the source term \mathbf{g} on the basis of these vectors, the original Eq. (1) simplifies to

$$\frac{\partial \mathbf{y}}{\partial t} = \mathbf{L} + \mathbf{a}_s \mathbf{f}^s, \quad (20)$$

where

$$\mathbf{f}^s = \mathbf{b}^s \cdot \mathbf{g}. \quad (21)$$

Equation (20) is accompanied by the following M algebraic equations:

$$\mathbf{f}^r = \mathbf{b}^r \mathbf{g} \approx \mathbf{0} \quad (22)$$

and the following E identity equations:

$$\mathbf{f}^c = \mathbf{b}^c \mathbf{g} \equiv \mathbf{0}. \quad (23)$$

The M algebraic Eqs. (22) express the steady-state and/or partial equilibrium approximations introduced and the E identity Eqs. (23) express the conservation of elements in the elementary steps of the detailed mechanism ($\mathbf{b}^i \cdot \mathbf{W}\mathbf{S}_j \equiv 0$). The reduced mechanism is formed by the second term in the RHS of Eq. (20). The $N - M - E$ vectors in \mathbf{a}_s are the stoichiometric vectors and the amplitudes in \mathbf{f}^s are the corresponding rates. When only steady state approximations are involved, they can always be expressed in the form of Eq. (22) and the stoichiometric vectors in \mathbf{a}_s involve only the $N - M$ non steady-state species. However, when partial equilibrium approximations are involved, they cannot always be expressed in that form and the reduced mechanism in Eq. (20) cannot be constructed [20]. In the case where partial equilibrium approximations can be cast in the form of Eqs. (22), the stoichiometric vectors in \mathbf{a}_s involve *all the* N species. This is the reason why steady state assumptions are most often encountered in the literature and will be used in the analysis that follows.

Let us assume that a global reduced mechanism is to be constructed on the basis of M steady state assumptions. Let us further assume that the M “steady-state” species and the corresponding M fast elementary reactions have been selected. The methodology for this selection is discussed in a section that follows. On the basis of these assumptions, the original Eq. (1) can be cast in the form:

$$\frac{\partial}{\partial t} \begin{bmatrix} \mathbf{y}_{ss} \\ \mathbf{y}_{ns} \end{bmatrix} = \begin{bmatrix} \mathbf{L}_{ss} \\ \mathbf{L}_{ns} \end{bmatrix} + \begin{bmatrix} \mathbf{g}_{ss} \\ \mathbf{g}_{ns} \end{bmatrix}, \quad (24)$$

where \mathbf{y}_{ss} and \mathbf{y}_{ns} are M and $N - M$ dimensional column vectors, the elements of which are the mass fractions of the “steady-state” and remaining (non steady or major) species, respectively. The vectors \mathbf{L}_{ss} , \mathbf{g}_{ss} , \mathbf{L}_{ns} , and \mathbf{g}_{ns} are defined accordingly. Then, the \mathbf{a}_i and \mathbf{b}^i vectors (18) and (19) are computed according to the following steps.

- (i) The M N -dimensional row vectors in \mathbf{b}^r have the form:

$$\mathbf{b}^r = [\mathbf{I}_{MM}, \mathbf{0}_{M(N-M)}] \quad (25)$$

where \mathbf{I}_{MM} is a $M \times M$ unit matrix and $\mathbf{0}_{M(N-M)}$ is a $M \times (N - M)$ zero matrix. With this definition, Eq. (22) yields $\mathbf{g}_{ss} = 0$, which express the steady-state assumptions for the M species in \mathbf{y}_{ss} .

- (ii) The E N -dimensional row vectors in \mathbf{b}^c correspond to the E elements in the detailed mechanism. Given the ordering of the species in Eq. (24), the N components of each vector in \mathbf{b}^c are set equal to the number of the elements in each of the N species divided by the corresponding molecular weight. In general, the $E \times N$ matrix \mathbf{b}^c is fully populated.
- (iii) The M N -dimensional column vectors in \mathbf{a}_r are computed from the relation:

$$\mathbf{a}_r = \mathbf{W}\mathbf{S}_r(\mathbf{b}^r\mathbf{W}\mathbf{S}_r)^{-1}, \quad (26a)$$

where \mathbf{S}_r is a $N \times M$ matrix whose columns are the stoichiometric vectors of the M reactions identified as fast. In order for the vectors in \mathbf{a}_r to be linearly independent, the vectors in \mathbf{S}_r must also be linearly independent. Furthermore, as Eq. (26a) shows, the stoichiometric vectors of the fast reactions must produce a matrix $\mathbf{b}^r\mathbf{W}\mathbf{S}_r$ that is invertible. With the ordering of the species as in Eq. (24) and the definition of \mathbf{b}^r , this means that the $M \times M$ matrix $\mathbf{S}_{r,ss}$ is invertible, where

$$\mathbf{W}\mathbf{S}_r = \begin{bmatrix} \mathbf{S}_{r,ss} \\ \mathbf{S}_{r,ns} \end{bmatrix} \quad (26b)$$

and $\mathbf{S}_{r,ns}$ is a $(N - M) \times M$ matrix. With this notation, the $N \times M$ matrix \mathbf{a}_r has the form:

$$\mathbf{a}_r = \begin{bmatrix} \mathbf{I}_{MM} \\ \mathbf{S}_{r,ns}\mathbf{S}_{r,ss}^{-1} \end{bmatrix}. \quad (26c)$$

- (iv) The computation of the $(N - M - E)$ N -dimensional row vectors in \mathbf{b}^s is executed in two steps. Given the $M + E$ row vectors in \mathbf{b}^r and \mathbf{b}^c , first the complementary linearly independent $N - M - E$ row vectors are determined and stored in, say, $\hat{\mathbf{b}}^s$. Note that this set of vectors is not unique. Then, a new set of vectors, say \mathbf{b}^s , is computed from the relation:

$$\mathbf{b}^s = \hat{\mathbf{b}}^s[\mathbf{I}_{NN} - \mathbf{a}_r\mathbf{b}^r], \quad (27)$$

where \mathbf{I}_{NN} is a $N \times N$ unit matrix. In general, the $(N - M - E) \times N$ matrix \mathbf{b}^s is fully populated.

- (v) Following, the matrix \mathbf{a} is computed from the equation:

$$\mathbf{a} = \begin{bmatrix} \mathbf{b}^r \\ \mathbf{b}^s \\ \mathbf{b}^c \end{bmatrix}^{-1} = [\mathbf{a}_r \quad \mathbf{a}_s \quad \mathbf{a}_c], \quad (28)$$

where \mathbf{a}_r is given by Eq. (26) and \mathbf{a}_s and \mathbf{a}_c have the form:

$$\mathbf{a}_s = \begin{bmatrix} \mathbf{0}_{M(N-M-E)} \\ \mathbf{a}_{s,ns} \end{bmatrix} \quad \mathbf{a}_c = \begin{bmatrix} \mathbf{0}_{ME} \\ \mathbf{a}_{c,ns} \end{bmatrix}, \quad (29)$$

where $\mathbf{0}_{M(N-M-E)}$ and $\mathbf{0}_{ME}$ are $M \times (N - M - E)$ and $M \times E$, respectively, zero matrices and $\mathbf{a}_{s,ns}$ and $\mathbf{a}_{c,ns}$ are $(N - M) \times (N - M - E)$ and $(N - M) \times E$ fully populated matrices. This form of \mathbf{a}_s and \mathbf{a}_c is the result of the particular structure of \mathbf{b}^r , Eq. (25), and the orthogonality condition (28).

Expanding the source term with respect to the above basis vectors, the original Eq. (1) becomes:

$$\begin{aligned} \frac{\partial}{\partial t} \begin{bmatrix} \mathbf{y}_{ss} \\ \mathbf{y}_{ns} \end{bmatrix} &= \begin{bmatrix} \mathbf{L}_{ss} \\ \mathbf{L}_{ns} \end{bmatrix} + \begin{bmatrix} \mathbf{I}_{MM} \\ \mathbf{S}_{r,ns}\mathbf{S}_{r,ss}^{-1} \end{bmatrix}(\mathbf{g}_{ss}) + \begin{bmatrix} \mathbf{0}_{MM} \\ \mathbf{a}_{s,ns} \end{bmatrix} \\ &\quad \cdot (\mathbf{b}^s\mathbf{W}\mathbf{S}\mathbf{R}) + \begin{bmatrix} \mathbf{0}_{MM} \\ \mathbf{a}_{c,ns} \end{bmatrix}(\mathbf{b}^c\mathbf{W}\mathbf{S}\mathbf{R}), \end{aligned} \quad (30)$$

where the notation of Eq. (24) has been used. By using the steady state assumptions introduced by Eq. (22) ($\mathbf{f}^r = \mathbf{b}^r\mathbf{g} = \mathbf{g}_{ss} = \mathbf{0}$) and the conservation of elements in the elementary reactions Eq. (23) ($\mathbf{b}^c\mathbf{W}\mathbf{S} = \mathbf{0}$), Eq. (30) simplifies to the form of Eq. (20) as

$$\frac{\partial}{\partial t} \begin{bmatrix} \mathbf{y}_{ss} \\ \mathbf{y}_{ns} \end{bmatrix} = \begin{bmatrix} \mathbf{L}_{ss} \\ \mathbf{L}_{ns} \end{bmatrix} + \begin{bmatrix} \mathbf{0}_{MM} \\ \mathbf{a}_{s,ns} \end{bmatrix}(\mathbf{b}^s\mathbf{W}\mathbf{S}\mathbf{R}). \quad (31)$$

A further simplification of this equation can be introduced by defining:

$$\mathbf{W}\mathbf{S} = [\mathbf{W}\mathbf{S}_r \quad \mathbf{W}\mathbf{S}_{k-r}] \quad \mathbf{R} = [\mathbf{R}_r \mathbf{R}_{k-r}], \quad (32)$$

where the columns of the $N \times M$ matrix \mathbf{S}_r are the M stoichiometric vectors of the M fast elementary reactions and the M dimensional vector \mathbf{R}_r contains the corresponding rates. The

$N \times (K - M)$ matrix \mathbf{S}_{k-r} and the $(K - M)$ dimensional vector \mathbf{R}_{k-r} contain the remaining stoichiometric vectors and rates in the detailed mechanism, respectively. By using the orthogonality condition (28) and the fact that the matrix $\mathbf{b}^s \mathbf{W}_r$ is by construction non-singular, it follows:

$$\mathbf{b}^s \mathbf{W}_r (\mathbf{b}^r (\mathbf{W}_s)_r)^{-1} = \mathbf{0} \Rightarrow \mathbf{b}^s \mathbf{W}_s = \mathbf{0} \quad (33)$$

Therefore, Eq. (31) simplifies to

$$\frac{\partial}{\partial t} \begin{bmatrix} \mathbf{y}_{ss} \\ \mathbf{y}_{ns} \end{bmatrix} = \begin{bmatrix} \mathbf{L}_{ss} \\ \mathbf{L}_{ns} \end{bmatrix} + \begin{bmatrix} \mathbf{0}_{MM} \\ \mathbf{a}_{s,ns} \end{bmatrix} (\mathbf{b}^s \mathbf{W}_s \mathbf{R}_{k-r}) \quad (34)$$

In practice, the global rates $\mathbf{b}^s \mathbf{W}_s \mathbf{R}_{k-r}$ are even further simpler than their expression shows. Actually, some of the columns in $\mathbf{W}_s \mathbf{R}_{k-r}$ are linearly dependent to the columns in \mathbf{W}_r . From Eq. (33) it follows that the rates of the corresponding elementary reactions do not show up in the expressions for the global rates. In any case, following the discussion of Eqs. (20–23), Eq. (34) shows that the $N - M - E$ stoichiometric vectors of the reduced mechanism do not involve the M “steady-state” species and the corresponding rates do not involve the M fast reactions. Given that the steady state assumption has been employed for the M species in \mathbf{y}_{ss} , only the last $N - M$ components of Eq. (34) are meaningful. Therefore, the original system of Eq. (1) is approximated by a set of M algebraic relations and $N - M$ differential equations:

$$\mathbf{b}^r \mathbf{g} = \mathbf{g}_{ss} = \mathbf{0} \quad (35)$$

$$\frac{\partial \mathbf{y}_{ns}}{\partial t} = \mathbf{L}_{ns} + \mathbf{a}_{s,ns} (\mathbf{b}^s \mathbf{W}_s \mathbf{R}_{k-r}) \quad (36)$$

from which the M “steady-state” and the remaining $N - M$ species are computed, respectively.

Even though the solutions for all the “steady state” species might not be wanted, they have to be computed in order to calculate the reaction rates in \mathbf{R}_{k-r} . Usually, this is performed with the method of “inner-iteration” (fixed point iteration) [41, 42]. However, when the detailed mechanism is quite complex, the steady-state species in \mathbf{y}_{ss} exceed by far in number the non steady ones in \mathbf{y}_{ns} ($M \gg N - M$). As a result, the solution of the M algebraic Eqs. (35) accounts for a large portion of the total computation time needed for the solution of the differ-

ential Eq. (36). This problem is generally faced with the simplification of the steady state relations $\mathbf{g}_{ss} = \mathbf{0}$ and the expressions for both the global rates $\mathbf{b}^s \mathbf{W}_s \mathbf{R}_{k-r}$. A significant simplification of the algebraic relations (35) might result in a weaker coupling among the relations and a much faster convergence of their solution, while a similar treatment of the global rates might make unnecessary the computation of all “steady state” species. Such simplifications can be identified using the concept of Importance and Participation indices, Eqs. (15) and (16). In particular, by defining two small positive numbers ϵ_P and ϵ_I , the elementary rates that produce $|P_j^m| < \epsilon_P$ ($m = 1, M$ $j = 1, K$) and $|I_j^n| < \epsilon_I$ ($n = 1, N$ $j = 1, K$) are neglected in the expressions for the steady state relations and global rates, respectively. Another answer to this problem is to tabulate all possible solutions of the steady state relations and use these tables for the computation of \mathbf{R}_{k-r} , a procedure already implemented with the ILDM approach [12–14] and improved with the use of orthogonal polynomials [43]. A further improvement in the efficiency of this approach is provided by the method of “in situ tabulation” recently developed by Pope [44].

In this section, an algorithm for constructing global reduced mechanisms was presented. Apart from the detailed mechanism, the algorithm requires as input the following additional information: (i) the number of steps in the reduced mechanism S ($= N - M - E$) and (ii) the M “steady-state” species and the corresponding M fast elementary reactions. The specific method for producing these data will be discussed next in the context of the analysis of a laminar premixed CH_4/Air flame.

LAMINAR PREMIXED CH_4/AIR FLAMES

We consider a one-dimensional, unstretched, premixed, laminar steady CH_4/Air flame. The unburned mixture enters at $x \rightarrow -\infty$ and the burnt gas exits at $x \rightarrow +\infty$. Assuming the Mach number of the flow to be low, the pressure is taken to be constant. On the basis of these assumptions, the governing equations for the conservation of the overall mass, species mass fraction and energy are

$$\rho u = \rho_u S_L \quad (37a)$$

$$\rho u \frac{dy^i}{dx} = -\frac{dj^i}{dx} + g^i \quad i = 1, N \quad (37b)$$

$$\rho u c_p \frac{dT}{dx} = \frac{d}{dx} \left(\lambda \frac{dT}{dx} \right) - \sum_{i=1}^N h_i g^i - \frac{dT}{dx} \sum_{i=1}^N c_{pi} j^i \quad (37c)$$

where ρ is the mixture density, u is the gas velocity, y^i is the species mass fraction, j^i is the diffusion flux, g^i is the chemical production rate, c_p is the specific heat of the mixture, T is the temperature, λ is the thermal conductivity, h_i is the enthalpy of formation, and N is the number of species [6, 45]. In Eq. (37a), the subscript “ u ” denotes the conditions in the unburned gas and S_L denotes the laminar burning velocity which is an eigenvalue and must be computed along with the numerical solution. Eqs. (37a–c) are accompanied by the ideal gas equation of state:

$$\frac{P}{\rho} = R^0 T \sum_{i=1}^N y^i / W_i \quad (38)$$

where P is the pressure, R^0 is the universal gas constant and W_i is the molecular weight of the i -th species. For boundary conditions we assume fixed values at the left boundary and zero fluxes at the right:

$$T = T_u \quad y_i = y_{iu} \quad \text{at } x \rightarrow -\infty, \quad (39)$$

$$\frac{dT}{dx} = 0 \quad \frac{dy_i}{dx} = 0 \quad \text{at } x \rightarrow +\infty. \quad (40)$$

The chemical kinetics of the problem is described by the GRI v2.11 mechanism, involving 279 elementary reactions, 49 species, and 5 elements ($K = 279$, $N = 49$, $E = 5$) and accounting for prompt and thermal NO_x formation [45]. Equations (38–41) were solved with the Cambridge Laminar Flame Code RUN-1DL [45] by using both the detailed and reduced mechanisms. For the latter case, the mass fractions of the “steady-state” species were computed with the method of “inner-iteration.” Unless otherwise specified, the results that will be analysed and reported next were obtained for the following operating conditions: the pressure is considered atmospheric (1 atm), the initial ($x \rightarrow -\infty$) temperature is taken to be

300K, the fuel is initially assumed to contain only CH_4 and the equivalence ratio φ is considered equal to 1.

Given the physical problem described by Eqs. (37–40) and the GRI v2.11 mechanism, the algorithm for constructing a global reduced mechanism, described previously, starts with the specification of the scalar M (or alternatively the number of global steps: $S = N - M - E$) and the identification of M “steady-state” species and an equal number of fast reactions. This identification process is described next.

IDENTIFICATION OF STEADY-STATE SPECIES AND FAST REACTIONS

Let us assume that it is desired to construct a seven-step global mechanism for the physical problem defined by Eqs. (37a–c) and the GRI detailed mechanism. For that purpose, $M = N - E - 7 = 37$ steady state assumptions must be introduced. That is, it is assumed that there exist 37 species which can be identified as “steady state” throughout the computational domain and that the trajectory moves along a 12-dimensional manifold in the 49-dimensional space of species’ mass fraction, defined by the corresponding 37 steady-state algebraic relations. In order to identify the 37 species which can be globally characterized as “steady state,” we first assume that the 37 algebraic relations forming the manifold are of the form of Eqs. (8), in which the vectors \mathbf{b}^i are provided by Eqs. (5a–d) and are functions of \mathbf{y} . On the basis of these relations, at each point in space all 49 species in the detailed mechanism are considered as candidates for being identified as globally “steady state.” This evaluation is based on the CSP-pointer, Eq. (14). Since a fixed M but variable vectors \mathbf{b}^i are employed, the set of 37 species which can be locally identified as “steady state” will vary with space; i.e., in a certain spatial subdomain a specie might be identified as “steady state” and in another subdomain as major. By recording at each grid point these local data, i.e., how close to be characterized as “steady state” are the 49 species, the 37 global such species can be identified. This local to global realization is executed as follows.

Having available the solution of Eqs. (37–40) on the basis of the detailed mechanism, the CSP

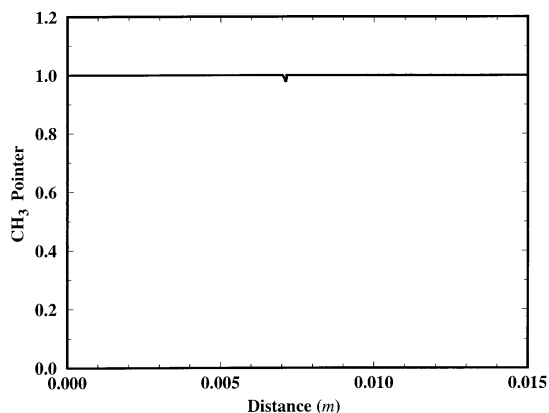


Fig. 1. The CSP-pointer D^i for the species CH_3 vs x ; $\varphi = 1$, $T_u = 300$ K, and $P = 1$ atm.

basis vectors (5a–d) are computed at each grid point and the N diagonal elements D^i of the “CSP-pointer”:

$$\mathbf{D} = \text{diag} \left[\mathbf{a}_1 \mathbf{b}^1 + \mathbf{a}_2 \mathbf{b}^2 + \cdots + \mathbf{a}_M \mathbf{b}^M \right] \quad (41)$$

are recorded, where \mathbf{D} is an N -dimensional vector. D^i are its elements, the superscript “ i ” refers to the i -th species in the detailed mechanism and their sum equals M . At each grid point, the elements of \mathbf{D} which are the closest to unity point to the species whose axes are the most perpendicular to the manifold and, therefore, are affected by the M fastest time scales. Following the discussion in the Introduction, the “steady state” species must be pointed by \mathbf{D} . As Fig. 1 shows, such a specie is CH_3 , for which the CSP-pointer D^{CH_3} is close to unity throughout the computational domain, even in the regions where its mass fraction and net production rate is negligible ($0 < x < 0.00675$ and $0.0075 < x < 0.01$). However, not all pointed species are good candidates for being globally “steady state.”

Consider for example the evolution in space of the pointer D^i for the species CH_4 , displayed in Fig. 2. It is shown that D^{CH_4} is practically zero ahead of the main reaction zone (located around $x = 0.0072$ m), rising to unity further down. This indicates that the 12-dimensional manifold is almost tangent to the axis of CH_4 before the main reaction zone, becoming perpendicular afterwards. The fact that $D^{\text{CH}_4} \approx 0$ ahead of the main reaction zone implies that

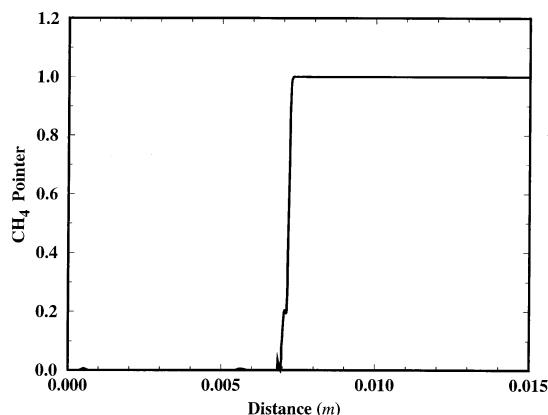


Fig. 2. The CSP-pointer D^i for the species CH_4 vs x ; $\varphi = 1$, $T_u = 300$ K, and $P = 1$ atm.

CH_4 is definitely a major specie there, since it is not affected by the M fastest time scales. However, the fact that $D^{\text{CH}_4} \approx 1$ inside the main reaction zone does not mean that CH_4 becomes a “steady-state” specie. It simply means that the time scale of its depletion is among the M fastest, its rate of depletion being much larger than that of production. Further down, where CH_4 has been completely depleted and the manifold passes through the origin, the fact that $D^{\text{CH}_4} \approx 1$ means that any perturbation in the CH_4 mass fraction off zero will decay with one of the M fastest scales. Since in that region its production rate is negligible, CH_4 can indeed be accurately computed by the appropriate steady state relation and therefore can indeed be characterized there as a “steady-state” specie. From the discussion above it is clear that, even though $D^{\text{CH}_4} \approx 1$ in a large portion of the computational domain, CH_4 cannot be characterized as globally “steady state,” since ahead and inside the main reaction zones it is a major specie.

Another misinterpretation that can be reached by inspecting the local values of the CSP-pointer alone is indicated by the evolution of D^{HCNO} , shown in Fig. 3. Both before and after the main reaction zone, where HCNO has either not been formed yet or it has been depleted, $D^{\text{HCNO}} \approx 0$. It is only in the main reaction zone where HCNO appears, where its mass fraction attains the maximum value of $1.0\text{e} - 7$. In the region before the main reaction zone, where HCNO has not been formed, the fact that $D^{\text{HCNO}} \approx 0$ there means that its

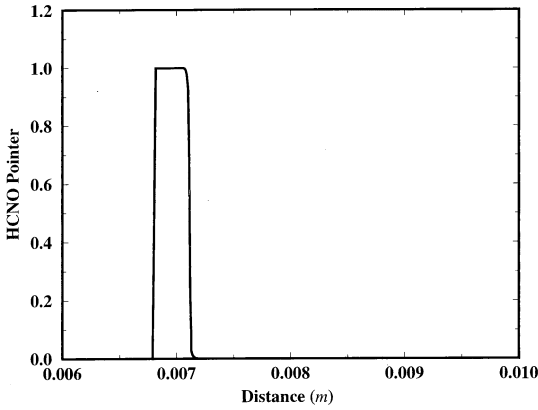


Fig. 3. The CSP-pointer D^i for the species HCNO vs x ; $\varphi = 1$, $T_u = 300$ K, and $P = 1$ atm.

evolution is characterized by a slow time scale. Therefore, HCNO cannot be formally characterized as “steady state” there. However, since its production rate there is negligible, it follows that HCNO can be accurately approximated by the steady-state relation. Similar conclusions can be drawn for the region behind the main reaction zone where HCNO has been depleted and $D^{\text{HCNO}} \approx 0$ also. Inside the main reaction zone, where the mass fraction of HCNO reaches its maximum value, Fig. 3 shows that $D^{\text{HCNO}} \approx 1$, indicating that it can be really considered as a “steady state” specie. The conclusion is that although HCNO produces $D^{\text{HCNO}} \approx 0$ in most of the computational domain, its mass fraction can be accurately computed by its steady-state relation everywhere.

From the results discussed above we conclude that the pointer **D** should not be considered alone when selecting the “steady-state” species. The possible misunderstandings that might be reached by examining **D** alone are clearly shown when the global “steady-state” species are selected by integrating the values of D^i over the computational domain L as

$$I_1^i = \frac{1}{L} \int_0^L D^i dx. \quad (42)$$

With such a global interpretation of the local data, the 37 species that produce the largest values of I_1^i could be characterized as “steady-state” while the remaining 12 species, which produce the smallest such values could be char-

TABLE 1

The species producing the 20 minimum values of I_1^i , I_2^i , I_3^i , and $1/cX_{i,\max}$ ^a

	I_1^i	I_2^i	I_3^i	$1/cX_{i,\max}$
20	C ₂ H ₂	C ₂ H ₂	CH ₂	HCO
19	NO ₂	HO ₂	HCO	CH ₃ OH
18	H	C ₂ H ₄	CH ₃ OH	C ₂ H ₂
17	OH	C ₂ H ₆	C ₂ H ₂	HO ₂
16	HCCOH	CH ₂ O	HO ₂	NO
15	NH ₃	HCN	C ₂ H ₄	C ₂ H ₄
14	CH₄	CH ₃	C ₂ H ₆	C ₂ H ₆
13	HOCN	O	CH ₂ O	CH ₂ O
12	H₂	H	CH ₃	H
11	O₂	OH	O	CH ₃
10	CO	NO	H	O
9	HNCO	CH₄	OH	H₂
8	NO	N₂O	CH₄	OH
7	H₂O	H₂	H₂	CO
6	HCN	O₂	CO₂	CH₄
5	CO₂	CO	CO	CO₂
4	HCNO	H₂O	N₂	H₂O
3	N₂O	CO₂	O₂	O₂
2	N₂	N₂	H₂O	N₂
1	AR	AR	AR	AR

^aThe horizontal double line separates the “steady state” species (upper part) from the major species (lower part). Species in bold: major species in the final seven-step mechanism (S₁–S₇).

acterized as major ones. The results shown on Table 1, where the 20 species producing the smallest values of I_1^i are listed, indicate that such a method for identifying the 12 major species (or alternatively the 37 “steady-state” species) leads to unrealistic choices. This conclusion can be easily reached by noticing that the fuel CH₄ is not among the ones listed in the lower 12 positions. Therefore, it would have been taken as globally “steady state” and not as a major specie, if the criterion (42) was adopted.

From the conclusions reached by inspecting the results in Figs. 1 to 3, it seems that a better criterion to identify the 12 global major species is to integrate the pointers D^i only along the domain where each of the i -th specie is present and its net production rate is meaningful. For that reason we adopt the integral:

$$I_2^i = \frac{1}{L} \int_0^L D^i \frac{1}{X^i + \epsilon_1} \frac{q^i}{q_{\max}^i + \epsilon_2} dx, \quad (43)$$

where

$$q^i = |g^i| = |S_1^i R^1 + \dots + S_K^i R^K|.$$

X^i is the mole fraction of the i -th species, the subscript “max” denotes the maximum value along the computational domain, and ϵ_1 and ϵ_2 are properly selected small positive numbers (e.g., $\epsilon_1 = 1e - 20$ and $\epsilon_2 = 1e - 50$) used in order to avoid the numerical problems when q_{\max}^i or X^i equal zero (i.e., inert species). The second term in the integral (43) relates to the criterion used by Peters for the selection of “steady-state” species [5, 47]. By using a diffusing scaling, Peters shows that inside the flame large values of this term correspond to relatively small net production rates, which related them to “steady-state” species. Incorporating both the CSP-pointer and Peter’s criterion in the integral (43) and considering them only in the region where each of the species is produced or depleted (guaranteed by the term q^i/q_{\max}^i), the reason of the small net production rate for each specie is taken into account. For example, when a relatively small net rate (large value of $1/X^i$) is associated to the M fastest chemical time scales [$D^i = O(1)$], then the computed large value of I_2^i can be associated with a “steady-state” specie, the net production rate of which is small due to cancellations occurring in its source term under the influence of the fast time scales. In contrast, when a relatively small net rate (large value of $1/X^i$ is related to the $N - M$ slowest chemical time scales ($D^i \ll 1$), then the value of I_2^i) will be small and the i -th specie will be identified as major, since it is unaffected by the fast scales and, therefore, its small net rate is not the result of large cancellations in its source term. The results obtained by the use of the integral I_2^i , listed on Table 1, show that the set of 12 species selected as major ones is very meaningful, represents the three subsets of chemistry included in the detailed chemistry (H/O, C, and N) and as it will be shown later leads to a very successful seven-step mechanism.

In order to demonstrate further the usefulness of the CSP pointer D^i , Table 1 also lists the results obtained by considering the integral:

$$I_3^i = \frac{1}{L} \int_0^L \frac{1}{X^i + \epsilon_1} \frac{q^i}{q_{\max}^i + \epsilon_2} dx, \quad (44)$$

which is the same as Eq. (43) but without the pointer D^i . As Table 1 shows, the identified set of major species (occupying the 12 bottom places in the list) will produce a reduced mechanism in which the slow N -chemistry is totally absent. As a consequence, very slowly varying species (e.g., NO) are considered as “steady state,” while species that are related to the fastest time scales (e.g., CH_3 ; see Fig. 1) are identified as major. Apparently, the inclusion of D^i is very important in accounting the influence of the fast scales when identifying the “steady state” species. As Table 1 shows, using as criterion the value of $1/cX_{\max}^i$ ($c = \sqrt{W_{N_2}/W_{i,N_2}}$), proposed by Peters [5, 47], the resulting identifications are similar to those provided by the integral I_3^i .

Having selected the 37 “steady-state” species on the basis of the integral (43), the corresponding fast elementary reactions are identified as follows. First, the “steady-state” specie y^i ($i = 1, M$) producing the largest value of I_2^i is selected and all the rates of the elementary reactions that tend to deplete that specie are integrated over the computational domain L :

$$H_k^i = \frac{1}{L} \int_0^L R_k dx, \quad (45)$$

where the subscript “ k ” denotes the elementary reactions consuming the specie y^i . The reaction that produces the largest value of H_k^i is identified as the fastest and its stoichiometric vector \mathbf{S}_i is positioned in the first column of the $N \times M$ matrix \mathbf{S}_r in Eq. (26a). The same procedure is followed for the “steady-state” species that produce the second, third and so on largest values of I_2^i . During this process, at each stage of identifying the next fast reaction care must be taken that its stoichiometric vector does not violate the linear independence of the columns in \mathbf{S}_r and the invertability of the matrix $\mathbf{S}_{r,ss}$, as discussed after Eq. (26a). If at a certain stage the selected stoichiometric vector violates these conditions, the reaction producing the second largest value of H_k^i must be selected as the appropriate fast reaction for the “steady-state” specie y^i .

With the M “steady state” species and corresponding fast reactions identified, the constant basis vectors \mathbf{a}_i and \mathbf{b}^i are computed according

to Eqs. (25–29). The reduced mechanism then is extracted from Eqs. (35–36). The process described above is based on an assumption for the value of the scalar M . A guide on how this value is selected is presented next.

NUMBER OF STEPS IN THE REDUCED MECHANISM

The selection of the number S of global steps in the reduced mechanism is a very important step. Of course, as this number gets smaller, the numerical calculations in which the reduced mechanism is implemented become faster while the accuracy decreases. Therefore, the number of global steps is a trade-off between speed and accuracy. At this point, no algorithmic method is known for an a priori selection of the value of S . A good indication in making a choice for S could have been the existence of a gap in the eigenvalues of the Jacobian \mathbf{J} of the source term \mathbf{g} . However, for the size of the detailed kinetics mechanism considered here such a gap cannot be identified, since \mathbf{J} produces 44 nonzero eigenvalues the magnitude of which varies almost evenly between 10^0 and 10^8 (1/sec).

Another good indication for the selection of S can be provided by the specific species which are not characterized as “steady state” and therefore do participate in the stoichiometry of the global steps. Although such a process for selecting S requires some intuition and experience from the part of the investigator, it was shown to be very helpful. For example, let us assume that we are interested in producing a series of global mechanisms including from six to ten steps. Using the method for identifying the “steady-state” species described above, each of these reduced mechanisms will contain in its stoichiometry the species displayed on Table 2. It is shown that the stoichiometry of a seven-step mechanism will involve the same species as that of a six-step mechanism with the addition of H. O will be added in a eight-step mechanism and CH_3 in a nine-step mechanism. Finally, in a ten-step mechanism CH_3 is replaced by CH_2O and HCNO is added.

From the results shown on Table 2, reasonable conclusions can be reached for the required number of steps in the reduced mecha-

TABLE 2
The Major Species for $S = 6$ to 10

$S = 6$	$S = 7$	$S = 8$	$S = 9$	$S = 10$
			CH3	HCNO
		O	O	CH2O
	H	H	H	O
OH	OH	OH	OH	H
CH4	CH4	CH4	CH4	OH
NO	NO	NO	NO	CH4
H2	H2	H2	H2	NO
N2O	N2O	N2O	N2O	H2
CO	CO	CO	CO	N2O
O2	O2	O2	O2	CO
H2O	H2O	H2O	H2O	O2
CO2	CO2	CO2	CO2	H2O
N2	N2	N2	N2	CO2
AR	AR	AR	AR	N2
				AR

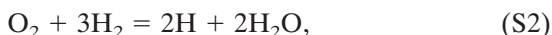
nism. When interested in modeling the combustion of a very rich mixture, in which case it is known that the C_2 chain becomes important, we have to use a mechanism involving more than ten steps. On the other hand, when a lean mixture is used a less than ten-step mechanism will be adequate. In the present investigation, seeking the minimum sized mechanism and knowing from the work of Peters and Bilger et al. [5, 32] that H is a major specie, the seven-step mechanism was selected to validate the algorithm presented here for the construction of global reduced mechanisms.

A SEVEN-STEP REDUCED MECHANISM

The methodologies discussed above for identifying the “steady-state” species and the fast elementary reactions, the construction of a global mechanism and the truncation of the expressions for the global rates, and the steady-state relations were implemented in the code S-STEP [48]. The required input to the code consists of (i) the detailed mechanism, (ii) the numerical solution of Eqs. (37–40) for a specific set of operating conditions, (iii) the number of global steps in the reduced mechanism, and if desired (iv) the small parameters ϵ_P and ϵ_I for the truncation process.

Inputting the GRI mechanism [46], the numerical solution for $P = 1$ atm, $T_u = 300$ K, $\varphi = 1$ and specifying $S = 7$ and $\epsilon_P = \epsilon_I = 0$, the

S-STEP code produced the following reduced mechanism:



in which Ar is included as an inert specie. The global rates of this mechanism are listed in Appendix I. S-STEP identified as “steady state” the species: O, HO₂, H₂O₂, C, CH, CH₂, CH_{2(S)}, CH₃, HCO, CH₂O, CH₂OH, CH₃O, CH₃OH, C₂H, C₂H₂, C₂H₃, C₂H₄, C₂H₅, C₂H₆, HCCO, CH₂CO, HCCOH, N, NH, NH₂, NH₃, NNH, NO₂, HNO, CN, HCN, H₂CN, HCNN, HCNO, HOCN, HNCO, and NCO. The corresponding steady-state relations are also listed in Appendix I. Given the numerical solution, specified above, the reduced mechanism S₁–S₇ was produced by S-STEP in about 1 min of CPU time on a HP-715.

Note that of the seven steps in the reduced mechanism, the first three involve O-H-chemistry (S₁–S₃), the next two involve C₁-chemistry (S₄–S₅), and the final two involve N-chemistry (S₆–S₇). The four steps S₁, S₂, S₄, and S₅ form the well known four-step mechanism for methane combustion developed by Peters [4–6, 47].

Since the mechanism (S₁–S₇) was produced with $\epsilon_P = \epsilon_I = 0$, none of the global rates or the steady state relations were truncated by the S-STEP code. However, the corresponding mechanism provided not very accurate numerical results. In order to improve the accuracy, possible truncations were sought by comparing the Participation and Importance Indices on the basis of the solution of the detailed and reduced mechanisms. It was found that, using the reduced mechanism solution, reaction number 237 [46] was producing in the beginning of the induction period a Participation Index in the steady state relation for H₂CN significantly larger than that produced by the detailed mechanism

calculations. Implementing this truncation, the accuracy of the reduced mechanism improved by a large degree. As the relations listed in Appendix I show, this was the only truncation implemented.

Using the reduced mechanism (S₁–S₇) it was shown that numerical solutions to the set of Eqs. (37–40) were obtained about four times faster than when using the detailed mechanism. This modest, relative to the number of major species in the reduced mechanism, decrease of CPU time is in agreement with the reasoning of Somers and De Goey [27]. They argued that the expected CPU savings cannot be realized since, when using a reduced mechanism all elementary rates are calculated and all “steady-state” species are computed from the algebraic relations by applying the “inner-iteration” loop, several times at each grid point. They concluded that only linear, in terms of the number of species in the mechanism, CPU time savings can be obtained. Since in the problem considered here there are 49 species in the detailed mechanism and 12 in the reduced mechanism (i.e., 49/12 = 4.08), the four times speed-up observed is consistent with the linear CPU time saving. The calculations were indeed accelerated when the global rates and steady-state relations were truncated by specifying $\epsilon_P, \epsilon_I \ll 1$. However, not all truncations were equally valid throughout the range of values of operating conditions (like that of the equivalence ratio ϕ). We decided to proceed in the validation of the reduced mechanism without implementing truncations that will speed up the “inner-iteration” calculations since it is now established that tabulation of the solutions to the steady state relations will result in much faster computations [13–15, 43, 44]. An estimation of the expected acceleration can be provided by the fact that for the problem considered here and by employing the seven-step reduced mechanism about 90% of the CPU time per Newton iteration was taken by the “inner-iteration” loops for the 37 “steady-state” species.

VALIDATION OF THE MECHANISM

Numerical results were obtained on the basis of Eqs. (37a–c) and the seven-step global mechanism

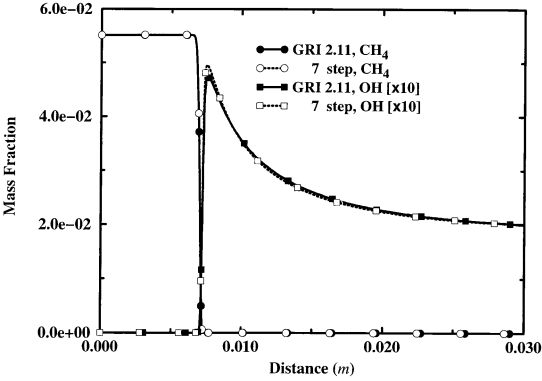


Fig. 4. The mass fraction of CH₄ and OH vs x ; $\varphi = 1$, $T_u = 300$ K, and $P = 1$ atm.

nism and were compared with those computed on the basis of the detailed mechanism [46]. Figures 4 and 5 show the evolution in space of the mass fraction of the species CH₄, OH, N₂O and NO all of which are major species appearing in the seven-step mechanism. This high accuracy is obtained over a wide range of values of the equivalence ratio φ . This is shown by the results displayed in Fig. 6 where the final ($x \rightarrow \infty$) mass fraction of NO is plotted against all possible values of φ . Similar accuracy is provided for all major species. However, this is not true for all “steady-state” species, the mass fractions of which are computed from the corresponding algebraic relations. Some of these species are predicted as accurately as the major species, while others are predicted accurately enough.

The seven-step mechanism produced very accurate values for the laminar burning velocity

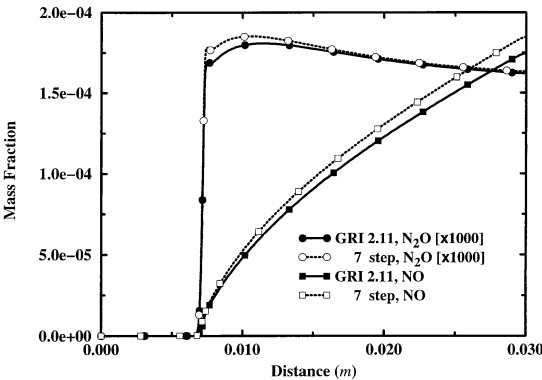


Fig. 5. The mass fraction of N₂O and NO vs x ; $\varphi = 1$, $T_u = 300$ K, and $P = 1$ atm.

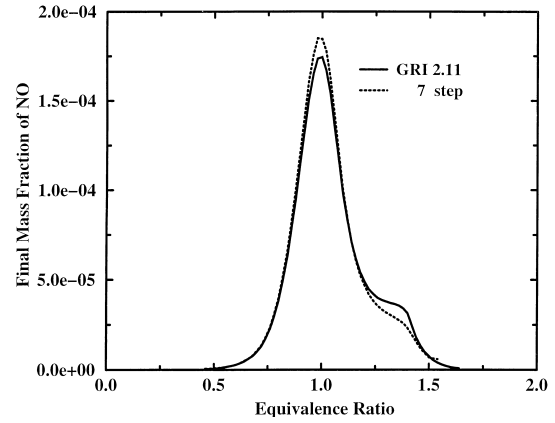


Fig. 6. The final mass fraction of NO vs φ ; $T_u = 30$ K and $P = 1$ atm.

S_L . This is shown in Figs. 7 and 8 for a wide range of values of the equivalence ratio φ and the initial temperature T_u . Moreover, the reduced mechanism predicted very accurately the temperature profile. This is shown in Figs. 9 and 10. Figure 9 displays the temperature profile for three values of φ while in Fig. 10 the variation of the final ($x \rightarrow \infty$) temperature is plotted against all possible values of φ .

It is clear that the reduced mechanism is very accurate for most quantities of interest for the whole range of values of φ and a wide range of T_u . This is a remarkable achievement considering that the analysis, on the basis of which the mechanism was constructed, was done only for $\varphi = 1$ and $T_u = 300$ K. This success is traced to the correct identification of the set of “steady

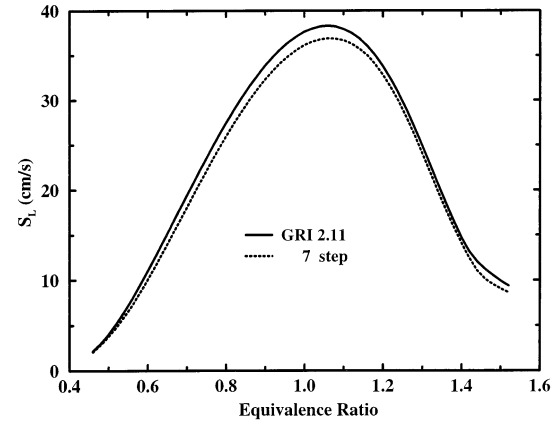


Fig. 7. The laminar burning velocity S_L vs φ ; $T_u = 300$ K and $P = 1$ atm.

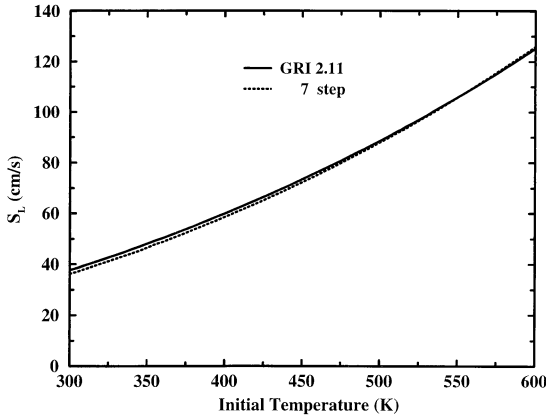


Fig. 8. The laminar burning velocity S_L vs T_u ; $\varphi = 1$ and $P = 1$ atm.

state” species, which apparently is valid for all values of φ and T_u .

ON THE IDENTIFICATION OF “STEADY-STATE” SPECIES

The criterion, Eq. (43), on the basis of which the “steady-state” species were identified combines the effects of the fast chemical time scales and those of the diffusive time scales. In essence, Eq. (43) attempts to identify as “steady state” those species which are affected the most by the M fastest chemical time scales but are associated with a slow diffusive time scale. The reason is the following.

When M such species are to be identified as

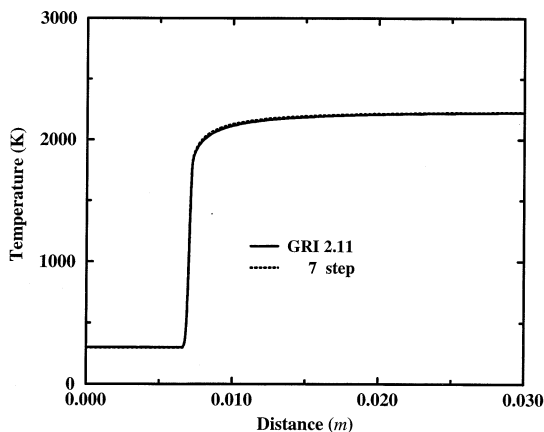


Fig. 9. The temperature vs x ; $\varphi = 1$, $T_u = 300$ K, and $P = 1$ atm.

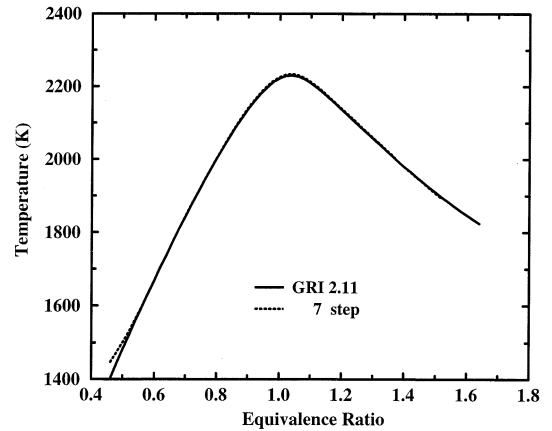


Fig. 10. The final temperature vs φ ; $T_u = 300$ K and $P = 1$ atm.

“steady state,” it is assumed that there exist M chemical time scales in the problem, say $\tau_{i,ch}$ ($i = 1, M$), which are much faster not only to the remaining $N - M$ chemical scales but also to M of the diffusive time scales, say $\tau_{j,d}$ ($j = 1, N$). For a successfully identified “steady state” specie:

$$\tau_{j-M_{\max},ch} \ll \tau_{j,d} \quad (46)$$

where the subscript $j - M_{\max}$ denotes the slowest of the M fastest chemical time scales characterizing the j -th specie. Obviously, when $\tau_{j,d} \gg \tau_{M_{\max},ch}$ this specie cannot be characterized as “steady state,” even though it might be pointed by the CSP-pointer D^j [e.g., $D^j = O(1)$]. Such a specie is H which, for the CH_4/Air flame considered here, produces $D^H = O(1)$ throughout the computational domain. However, it is associated with a fast diffusion time scale and is identified as a major specie. The ideal situation in constructing a reduced mechanism is to identify M species which produce $D^j = O(1)$ and satisfy Eq. (46). However, such an event is very difficult to encounter, especially when the detailed mechanism is complex and the specified scalar M is large. In such a case, the most successful criterion for selecting the M “steady-state” species seems to be the magnitude of the ratio $\tau_{j-M_{\max},ch}/\tau_{j,d}$. The smallest the value of this ratio, the most likely is for the j -th specie to be a “steady-state” one. This issue is the subject of further research.

Note that the difficulty in identifying the

“steady state” species is surfacing only when the scalar M is fixed. When the scalar M is allowed to vary with time and space, the local identification of the “steady-state” species is entirely based on the CSP-pointer, Eq. (14). This is due to the fact that with the criterion for detecting the exhausted modes, Eq. (7), only the chemical time scales which satisfy Eq. (46) are considered fast [12]. As a result, the algebraic Eqs. (22) are solved for the concentration of the species, which produce the largest values of D^i .

SLOW VARYING PROGRESS VARIABLES AND CONSERVED SCALARS

The constant vectors \mathbf{a}_r , \mathbf{a}_s , \mathbf{a}_c , \mathbf{b}^r , \mathbf{b}^s , and \mathbf{b}_c , Eqs. (18 and 19), on the basis of which the global reduced mechanism is constructed, can serve in two important additional aspects. First, they can be the initial guess for the CSP vectors (5a–d) in the case where higher accuracy is desired and a local reduced mechanism of variable form, but with a fixed size, is to be used. In addition, they allow the reduced problem defined by Eqs. (35–36) to be cast in a more convenient form, for both laminar and turbulent flow calculations. Noting that the differential operator \mathbf{L} is linear in \mathbf{y} , a new set of unknowns can be defined as

$$\boldsymbol{\eta}^s = \mathbf{b}^s \mathbf{y} \quad \boldsymbol{\eta}^c = \mathbf{b}^c \mathbf{y}, \quad (47)$$

where $\boldsymbol{\eta}^s$ and $\boldsymbol{\eta}^c$ are $(N - M - E)$ and E -dimensional vectors, respectively. For the CH_4/Air problem considered here, the corresponding to the seven-step mechanism (S_1 – S_7) 7 vectors in \mathbf{b}^s and 5 in \mathbf{b}^c are listed in Appendix II along with the vector \mathbf{y} . The seven and five, respectively, variables in $\boldsymbol{\eta}^s$ and $\boldsymbol{\eta}^c$ can be defined by Eqs. (47). They are similar to the progress variables and conserved scalars, respectively, used in the simulation of turbulent combustion [49–51]. These variables are also related to the low dimensional set of variables used by the ILDM method [13–15]. The evolution of the progress variable $\eta^{38} = \mathbf{b}^{38} \cdot \mathbf{y}$ and the conserved scalar $\eta^{46} = \mathbf{b}^{46} \cdot \mathbf{y}$ (corresponding to the conservation H atoms), is displayed on Fig. 11. The effects of large diffusivities of the H and H_2 species is clearly demonstrated. On the basis of these new unknowns and assum-

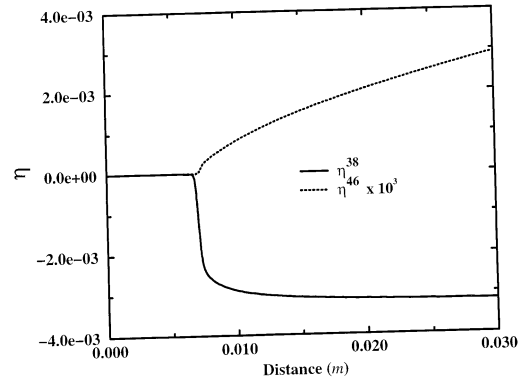


Fig. 11. The progress variable $\eta^{38} = \mathbf{b}^{38} \cdot \mathbf{y}$ and the conserved scalar $\eta^{46} = \mathbf{b}^{46} \cdot \mathbf{y}$; $\varphi = 1$, $T_u = 300$ K, and $P = 1$ atm.

ing equal diffusivities, the reduced problem, Eqs. (35–36), becomes

$$\mathbf{b}^r \mathbf{g} = \mathbf{g}_{ss} = \mathbf{0}, \quad (48)$$

$$\frac{\partial \boldsymbol{\eta}^s}{\partial t} = \mathbf{L}(\boldsymbol{\eta}^s) + (\mathbf{b}^s \mathbf{W} \mathbf{S}_{k-r} \mathbf{R}_{k-r}), \quad (49)$$

$$\frac{\partial \boldsymbol{\eta}^c}{\partial t} = \mathbf{L}(\boldsymbol{\eta}^c). \quad (50)$$

Following the discussion on the algorithm for producing the constant \mathbf{a}_i and \mathbf{b}^i vectors, the differential Eqs. (49) are free of the fastest chemical time scales in the problem. This is guaranteed by the fact that the elementary reactions related to the fastest scales are absent from the source term. As a result, these equations are less stiff than if an arbitrary set of such vectors was used. For the CH_4/Air flame considered here, this is demonstrated in Fig. 12 where the 1-st and 38-th eigenvalues, $\lambda_{1,f}$ and $\lambda_{38,f}$ respectively, of the full kinetics term in Eq. (1a) are displayed along with the 1-st eigenvalue $\lambda_{1,r}$ of the reduced kinetics term in Eq. (49). It is shown that the fastest chemical time scale ($1/\lambda$) of the reduced set of Eqs. (49) is much slower than that produced by the full source term. In fact, it is of the order of the 38-th chemical time scale of the full problem, i.e., given that $M = 37$, is of the order of the fastest time scale of the slow subdomain of \mathbf{y} . It is clear that the use of these $\boldsymbol{\eta}^s$ and $\boldsymbol{\eta}^c$ will facilitate the incorporation of global reduced mechanisms in turbulent combustion calculations.

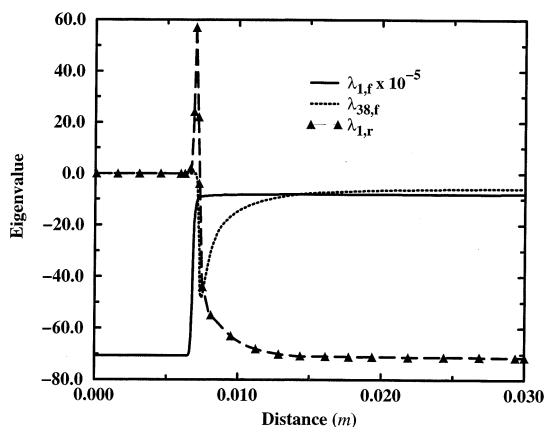


Fig. 12. The 1st (largest) and 38th eigenvalues of the Jacobian of the full source term ($\lambda_{1,f}$ and $\lambda_{38,f}$) and the 1st (largest) eigenvalue of the Jacobian of the reduced source term ($\lambda_{1,r}$) vs x .

CONCLUSIONS

An algorithmic procedure for the construction of global reduced chemical kinetic mechanisms was developed and implemented in the code S-STEP. As an example a very successful seven-step mechanism was constructed for the case of CH_4/Air laminar premixed flames accounting for prompt and thermal NO_x production. The algorithm is fully automated, uses a number of steady-state assumptions, implements concepts from the CSP method and requires a small amount of computations. Therefore, it is very much suited for the reduction of large and complex detailed mechanisms, such as those for heavy hydrocarbons.

The input to the algorithm that must be provided consists of (i) the detailed mechanism, (ii) the numerical solution of the problem under study for a specific set of operating conditions in the neighborhood of which the reduced mechanism is expected to be valid, and (iii) the desired number of global steps in the reduced mechanism. The output consists of the global steps, the corresponding global rates, which are linear relations among the elementary ones, the steady state relations and of course the constant basis vectors in \mathbf{a}_r , \mathbf{a}_s , \mathbf{a}_c , \mathbf{b}^r , \mathbf{b}^s and \mathbf{b}^c , Eqs. (18 and 19).

Given the input above, the algorithm in the S-STEP code constructs the reduced mecha-

nism in four steps. First, the “steady-state” species are identified. These are species which do not appear in the global steps and their mass fraction (if needed) is computed from algebraic relations. These species are identified with the help of the CSP-pointer, properly weighted and integrated over the computational domain. The second step consists of the identification of the fast elementary reactions which do not appear in the expressions for the global rates. These are identified among the reactions which consume most the “steady-state” species. Such an identification is possible by integrating over the computational domain all consuming elementary rates. In the selection of the fast reactions, care must be taken so that their stoichiometric vectors are linearly independent and that the matrix consisting of their stoichiometric coefficients of the “steady-state” species is invertible. With the “steady-state” species and the fast elementary reactions identified, the algorithm proceeds to the construction of the reduced mechanism, employing very simple linear algebra computations. The final step consists of the simplification (truncation) of the steady-state relations and the expressions of the global rates, with the purpose of making the solution to problems where the reduced mechanism is implemented faster to compute. This step is executed with the help of the Participation and Importance indices.

Our experience is that the most crucial steps in the construction of reduced mechanisms is the specification of the number of global reactions in the reduced mechanism and the identification of the “steady-state” species. For the first step no algorithmic method was found, although a guide for the selection of the desired number of global reactions was provided. This number must be a compromise between the needs of accuracy and simplicity of the mechanism (i.e., smallest possible number of steps). For the second step, the proposed algorithm based on the CSP-pointer and Peters criterion, Eq. (43), was shown to be very robust. Apart from its use in the CH_4 -Air case reported here, it was also employed successfully in the case of an H_2 -Air flame. However, since its development was based on physical arguments and not on a formal mathematical analysis, this part of the algorithm might need further investigation.

As an example of the implementation of the proposed algorithm for constructing reduced mechanisms, a seven-step mechanism was developed for the case of CH_4/Air laminar premixed flames from a detailed one consisting of 279 elementary reactions and 49 species. It was shown that the mechanism is very accurate for lean and rich flames as well as low and high initial temperatures, reproducing the most significant results including NO_x formation. As expected, the seven-step mechanism was shown to result in much faster calculations. However, a large portion of the computing time was taken for the computation of the “steady-state” species’ mass fraction with the method of “inner-iteration.” It is expected that the simulations can become much faster if the “inner-iteration” part of the code is replaced by tabulated solutions of the “steady-state” species from the corresponding algebraic relations.

The real advantage of the algorithmic procedure for constructing reduced mechanisms developed here is that it is simple and requires a very small amount of computations. Therefore, for a given type of flame, several reduced mechanisms can be developed depending on the operating conditions (e.g., inlet mixture composition, inlet temperature, pressure, etc.). Furthermore, the fact that the construction of the reduced mechanism is based on the “integration” of local CSP data (i.e., Eq. 43), indicates that the algorithm can be used for any flame geometry. This feature further suggests that a representative solution might not be needed as input to the algorithm. Such a development of the algorithm should be based on the availability of all possible states of the solution vector and of an appropriate “integration” method which will produce the global identifications required from the “local” dynamics data. This subject is now under study.

The assistance of Mr. N. Vassilopoulos and Dr. Y. Katsabanis in the development of some sections of the S-STEP code is gratefully acknowledged. Parts of the work were supported by the E.U. ESPRIT program “Development of a Turbulent Combustion Code for Industrial Application (TANIT)” Co. no. 8835.

REFERENCES

1. Smooke M. D., Mitchell R. E., and Keyes D. E., *Combust. Sci. Tech.* 67:85–122 (1989).
2. Tomlin A., Turanyi T., and Pilling M., in *Oxidation Kinetics and Autoignition of Hydrocarbons* (M. Pilling, Ed.), Elsevier, New York, 1997, p. 293.
3. Fotache C. G., Kreutz T. G., and Law C. K., Ignition of Counter flowing Methane versus Heated Air Under Reduced and Elevated Pressures, *Combust. Flame* 108:442 (1997).
4. Peters N., in *Lecture Notes in Physics*, (Glowinski et al., Eds.), Springer, Berlin, 1985, p. 90.
5. Peters N., in *Fluid Dynamical Aspects of Combustion Theory*, (M. Onofri and A. Tesei, Eds.), Longman, 1990, p. 232.
6. Smooke M. D. (Ed.), *Reduced Kinetic Mechanisms and Asymptotic Approximations for Methane-Air Flames*, Lecture Notes in Physics, vol. 384, Springer, Berlin, 1991.
7. Peters N., and Rogg B. (Eds.), *Reduced Kinetic Mechanisms for Applications in Combustion Systems*, Springer Verlag, Berlin, 1993.
8. Lam S. H., and Goussis D. A., *22nd Symposium (Intl) on Combustion*, The Combustion Institute, Pittsburgh, 1988, p. 931.
9. Lam S. H., and Goussis D. A., in *Reduced Kinetic Mechanisms and Asymptotic Approximations for Methane-Air Flames*, (M. Smooke, Ed.), Springer Lecture Notes 384, 1991, p. 227.
10. Lam S. H., and Goussis D. A., *Intl. J. Chem. Kinetics* 26:461 (1994).
11. Lam S. H., *Combust. Sci. Tech.* 89:375 (1993).
12. Hadjinicolaou M., and Goussis D. A., *SIAM J. Sci. Comp.* 20:781 (1999).
13. Maas U., and Pope S. B., *Comb. Flame* 88:239 (1992).
14. Maas U., and Pope S. B., *24th Symposium (Intl) on Combustion*, The Combustion Institute, Pittsburgh, 1992, p. 103.
15. Maas U., and Pope S. B., *Twenty-fifth Symposium (Intl) on Combustion*, The Combustion Institute, Pittsburgh, 1994, p. 1349.
16. Niemann H., Schmidt D., and Maas U., *J. Eng. Math.* 31:131 (1997).
17. Eggels R. L. G. M., and de Goey L. P. H., *Comb. Flame* 100:559 (1995).
18. Rouchon P., Report CAS-ENSMP, Ecole des Mines de Paris, France, 1993.
19. Duchene P., and Rouchon P., *Chem. Eng. Sci.* 51:4661 (1996).
20. Goussis D. A., *J. Comp. Physics* 128:261 (1996).
21. Katsabanis Y., Ph.D. thesis, University of Patras, Greece, 1996.
22. Williams F. A., *Combustion Theory*, Benjamin-Cummings Publ., Boston, 1995.
23. Chen J. Y., A General Procedure for Constructing Reduced Reaction Mechanisms with Given Independent Relations, *Combust. Sci. Tech.* 57:89 (1988).
24. Goettgens J., Terhoeven P., and Korff R., RedMech, public domain code, techmech.ITM.RWTH-Aachen.DE, RWTH, Aachen, 1992.

25. Peters N., and Kee R. J., *Combust. Flame* 68:17 (1987).
26. Rogg B., in *Reduced Kinetic Mechanisms and Asymptotic Approximations for Methane-Air Flames*, (M. Smooke, Ed.), Springer Lecture Notes 384, 1991, p. 159.
27. Somers L. M. T., and De Goey L. P. H., *Twenty-fifth Symposium (Intl.) on Combustion*, The Combustion Institute, Pittsburgh, 1994, p. 957.
28. Turanyi T., Bérecs T., and Vajda S., *Intl. J. Chem. Kinet.* 21:83 (1989).
29. Tomlin A. S., Pilling M. J., Turanyi T., Merkin J. H., and Brindley J., *Combust. Flame* 91:107 (1992).
30. Hessler J. P., and Ogren P. J., *J. Chem. Phys.* 97:6249 (1992).
31. Jones W. P., and Lindstedt R. P., *Combust. Flame* 73:233 (1988).
32. Bilger R. W., Straner S. H., and Kee R. J., *Combust. Flame* 80:135 (1990).
33. Chang W. C., and Chen J. Y., 8-Step Reduced Mechanism for Methane, 1996, <http://firefly.berkeley.edu/griREDU.html>, Berkeley CA, USA.
34. Goussis D. A., and Lam S. H., *Proc. Twenty-fourth Symposium (Intl.) on Combustion*, The Combustion Institute, Pittsburgh, 1992, p. 113.
35. Katsabanis Y., and Goussis D. A., in *Combustion Technologies for a Clean Environment*, (S. Samuelson et al., Eds.), Gordon and Breach, 1997.
36. Fotache C. G., Kreutz T. G., and Law C. K., *Combust. Flame* 110:429 (1997).
37. Trevino C., and Mendez F., *Twenty-fourth Symposium (Intl.) on Combustion*, The Combustion Institute, Pittsburgh, 1992, p. 121.
38. Trevino C., and Mendez F., *Combust. Sci. Tech.* 78:197 (1992).
39. Goussis D. A., Lam S. H., and Gnoffo P. A., 28th AIAA Aerospace Sciences Meeting, paper 90-0644, Nevada, 1990.
40. Valorani M., and Goussis, D. A., submitted for publication, (1997).
41. Rogg B., and Williams F. A., Structures of Wet CO Flames with Full and Reduced Kinetics Mechanisms, *Twenty-second Symposium (Intl.) on Combustion*, The Combustion Institute, Pittsburgh, 1988, p. 1441.
42. Wang W., and Rogg B., *Combust. Flame* 94:271 (1993).
43. Turanyi T., *Computer Chem.*, 18:45 (1994).
44. Pope S. B., *Combust. Th. Modelling*, 1:41 (1997).
45. Rogg B., A Computer Program for the Simulation of One-Dimensional Chemically Reacting Flows, Report CUED/A-THERMO/TR39, Cambridge University, 1991.
46. Bowman C. T., Hanson R. K., Davidson D. F., Gardiner W. C., Lissianski V., Smith G. P., Golden D. M., Frenklach M., and Goldenberg M., GRI 2.11 Detailed Mechanism, http://www.me.berkeley.edu/gri_mech/, Berkeley CA, USA.
47. Peters N., in *Reduced Kinetic Mechanisms and Asymptotic Approximations for Methane-Air Flames* (Smooke M. D., Ed.) Lecture Notes in Physics vol. 384, Springer, Berlin, 1991, p. 48.
48. Vassilopoulos N., Massias Th., Katsabanis Y., and Goussis D. A., S-STEP Code, Report for the ESPRIT program, Co. no. 8835, 1996.
49. Bilger R. W., in *Turbulent Reacting Flows* (Libby P. A., and Williams F. A., Eds.), Springer Verlag, 1980.
50. Libby P. A., and Williams F. A., *AIAA J.* 19:261 (1981).
51. Sion M., and Chen J. C., *Combust. Sci. Tech.* 88:89 (1992).

Received 5 January 1998; revised 29 July 1998; accepted 25 August 1998

Appendices I and II at the following page.

APPENDIX I: THE GLOBAL RATES AND STEADY-STATE RELATIONS

Global rates (subscripts refer to the reactions in the GRI v2.11 mechanism [46]):

$$w_1 = 0.25[-6R_1 - 6R_2 - 2R_3 - 6R_4 - 3R_6 + R_7 - 3R_8 + R_9 - 3R_{11} - 5R_{12} - 6R_{13} - 5R_{14} - 2R_{15} - 6R_{16} - 6R_{17} + 4R_{20} - 3R_{22} + 3R_{23} + 3R_{24} + 4R_{25} - 6R_{27} + 4R_{28} - 9R_{29} - 5R_{30} + R_{31} + 4R_{32} - 4R_{39} - 4R_{40} - 4R_{41} - 4R_{42} - 3R_{43} - 3R_{44} - 4R_{45} - 6R_{46} + 2R_{47} - 3R_{48} - 3R_{50} - 3R_{52} - R_{53} - 4R_{54} - 4R_{55} - 6R_{59} - 4R_{60} - 6R_{61} - 6R_{62} - 6R_{63} - 4R_{65} - 6R_{66} - 6R_{67} + 2R_{68} + 2R_{69} - 3R_{70} - 4R_{72} - 4R_{73} - 4R_{77} - 4R_{78} + 3R_{79} - 7R_{80} - 3R_{81} + 9R_{82} + R_{84} + 3R_{86} - 3R_{87} + 3R_{88} + 3R_{89} - R_{90} + 3R_{91} + 3R_{92} + R_{93} + 3R_{94} + R_{99} - 3R_{100} + R_{101} - 3R_{102} - 3R_{103} + 3R_{104} + 3R_{105} + 3R_{106} + 9R_{107} + 6R_{110} - 3R_{111} + R_{112} - 3R_{113} - 6R_{114} - 6R_{115} - 6R_{116} - 3R_{117} - 3R_{118} - 5R_{120} - 2R_{121} - R_{122} - 7R_{123} - 7R_{124} + 3R_{125} + 2R_{127} - 6R_{128} - 3R_{129} - 4R_{130} - 7R_{131} + 2R_{132} - 3R_{134} + R_{135} + R_{136} - 6R_{137} - 3R_{138} + R_{141} + R_{144} - 2R_{145} + R_{146} - 3R_{149} + 2R_{153} - 3R_{154} + 6R_{155} + 3R_{157} - 3R_{160} + R_{161} + 3R_{162} + 3R_{163} + R_{164} - 3R_{165} + 7R_{171} + R_{172} + 6R_{173} + 4R_{176} + 4R_{177} - 3R_{181} - 3R_{182} - 3R_{183} + 3R_{184} + 3R_{185} - 6R_{186} - 6R_{187} - 3R_{190} - R_{191} - R_{192} - R_{194} - 3R_{195} - 3R_{196} - 2R_{197} - 3R_{198} - 2R_{200} - 3R_{201} + R_{203} - 6R_{207} - 3R_{208} - 4R_{209} - 3R_{210} - 3R_{211} - 4R_{212} - 2R_{213} + R_{215} + 4R_{216} + 3R_{218} + 3R_{220} + R_{221} - 3R_{222} + 3R_{224} - 3R_{225} - 2R_{226} + 3R_{227} - 2R_{229} + 3R_{230} - 3R_{233} + 2R_{235} + 2R_{236} - 4R_{238} - R_{239} + R_{242} + R_{243} - R_{244} - R_{245} + 3R_{248} - 2R_{250} - 2R_{253} - 2R_{255} + R_{256} - 3R_{257} - 6R_{258} + 3R_{259} + 3R_{260} - 4R_{261} - R_{262} - 3R_{263} - 2R_{264} + R_{267} + R_{268} + 4R_{269} - 2R_{271} + 2R_{273} + 3R_{274} + R_{275} - 3R_{276} - R_{277} - 3R_{279}]$$

$$w_2 = 0.25[2R_1 + 2R_2 + 2R_3 + 2R_4 + 5R_6 + 5R_7 + 5R_8 + 5R_9 + R_{11} + 3R_{12} + 2R_{13} + 3R_{14} + 6R_{15} + 2R_{16} + 2R_{17} + 4R_{20} + R_{22} + 3R_{23} - R_{24} + 4R_{25} + 2R_{27} + 8R_{28} + 3R_{29} + 7R_{30} + R_{31} + 4R_{32} + R_{43} + R_{44} + 2R_{46} - 2R_{47} + R_{48} + R_{50} + R_{52} - R_{53} - 4R_{54} + 4R_{58} + 2R_{59} + 2R_{61} + 2R_{62} + 2R_{63} + 2R_{66} + 2R_{67} - 2R_{68} - 2R_{69} + R_{70} + 3R_{79} + R_{80} + 5R_{81} - 3R_{82} - 4R_{83} + R_{84} - R_{86} + R_{87} - R_{88} - R_{89} + 3R_{90} + 3R_{91} - R_{92} + R_{93} - R_{94} + R_{99} + R_{100} + 5R_{101} + R_{102} + R_{103} - R_{104} - R_{105} - R_{106} - 3R_{107} + 2R_{110} + R_{111} + R_{112} + R_{113} + 2R_{114} + 2R_{115} + 2R_{116} + R_{117} + R_{118} + 3R_{120} + 6R_{121} + 3R_{122} + R_{123} + R_{124} + 3R_{125} - 2R_{127} + 2R_{128} + R_{129} - 3R_{131} + 2R_{132} + 5R_{134} + 5R_{135} + R_{136} + 2R_{137} + R_{138} - 4R_{140} + 5R_{141} + 5R_{144} + 6R_{145} + R_{146} + R_{149} - 2R_{153} + R_{154} - 2R_{155} - R_{157} + R_{160} + 5R_{161} - R_{162} - R_{163} + R_{164} + R_{165} + 7R_{171} + R_{172} + 2R_{173} + 8R_{176} + 8R_{177} + R_{181} + R_{182} + R_{183} - R_{184} - R_{185} + 2R_{186} + 2R_{187} + 5R_{190} + 3R_{191} + 3R_{192} + 4R_{193} + 3R_{194} + 5R_{195} + 5R_{196} + 2R_{197} + 5R_{198} + 4R_{199} + 2R_{200} + 5R_{201} + R_{203} + 2R_{207} - 3R_{208} + R_{210} + R_{211} + 2R_{213} + R_{215} + 4R_{217} - R_{218} - R_{220} + R_{221} + 5R_{222} + 3R_{224} + 5R_{225} + 6R_{226} + 3R_{227} + 4R_{228} + 6R_{229} - R_{230} + R_{233} - 2R_{235} - 2R_{236} - R_{239} - 3R_{242} - 3R_{243} - R_{244} + 3R_{245} + 3R_{248} + 2R_{250} + 2R_{253} + 2R_{255} + R_{256} + 5R_{257} + 2R_{258} + 3R_{259} + 3R_{260} + 3R_{262} + 5R_{263} + 2R_{264} + 2R_{267} + R_{268} + 2R_{271} - 2R_{273} + 3R_{274} + R_{275} + R_{276} - R_{277} + R_{279}]$$

$$w_3 = 0.25[2R_1 + 2R_2 + 2R_3 + 2R_4 - R_6 - R_7 - R_8 - R_9 + 3R_{11} + R_{12} + 2R_{13} + R_{14} + 2R_{15} + 2R_{16} + 2R_{17} + 3R_{22} + 2R_{23} + R_{24} + 2R_{27} + R_{29} + R_{30} - R_{31} - R_{43} - R_{44} + 2R_{46} - 2R_{47} - R_{48} - R_{50} - R_{52} + R_{53} + 2R_{59} + 2R_{61} + 2R_{62} + 2R_{63} + 2R_{66} + 2R_{67} - 2R_{68} - 2R_{69} - R_{70} + R_{79} - R_{80} - R_{81} - R_{82} - R_{84} - 3R_{86} - R_{87} - 3R_{88} - 3R_{89} - 3R_{90} - 3R_{91} - 3R_{92} - R_{93} - 3R_{94} - R_{99} - R_{100} - R_{101} - R_{102} - R_{103} - 3R_{104} - 3R_{105} - 3R_{106} - R_{107} - 2R_{110} - R_{111} - R_{112} - R_{113} - 2R_{114} + 2R_{115} + 2R_{116} - R_{117} - R_{118} + R_{120} + 2R_{121} - 3R_{122} - R_{123} - R_{124} - 3R_{125} - 2R_{127} - 2R_{128} - R_{129} - R_{131} - 2R_{132} - R_{134} - 2R_{135} - R_{136} - 2R_{137} - R_{138} - R_{141} - R_{144} - 2R_{145} - R_{146} - R_{149} - 2R_{153} - R_{154} - 2R_{155} - 3R_{157} - R_{160} - R_{161} - 3R_{162} - 3R_{163} - R_{164} - R_{165} - 3R_{171} - R_{172} - 2R_{173} + R_{181} + R_{182} + R_{183} - R_{184} - R_{185} + 2R_{186} + 2R_{187} - R_{190} - 3R_{191} - 3R_{192} - 4R_{193} - 3R_{194} - R_{195} - R_{196} - 2R_{197} - R_{198} - 2R_{199} + 2R_{200} - R_{201} - R_{203} + 2R_{207} + 3R_{208} - R_{210} - R_{211} + 2R_{213} - R_{215} - 4R_{217} - 3R_{218} - 3R_{220} - R_{221} - R_{222} - 3R_{224} - R_{225} - 2R_{226} - 3R_{227} - 2R_{228} - 2R_{229} + R_{230} + 3R_{233} - 2R_{235} - 2R_{236} + R_{239} + 3R_{242} + 3R_{243} + R_{244} - 3R_{245} - 3R_{248} + 2R_{250} + 2R_{253} + 2R_{255} + 3R_{256} - R_{257} + 2R_{258} - 3R_{259} - 3R_{260} + R_{262} - R_{263} + 2R_{264} - R_{267} - R_{268} + 2R_{271} - 2R_{273} + R_{274} + 3R_{275} + 3R_{276} + R_{277} + 3R_{279}]$$

$$w_4 = R_{12} + R_{14} + R_{30} + R_{31} + R_{99} + R_{120} - R_{132} - R_{153} + R_{226} + R_{229} + R_{262} + R_{268}$$

$$w_5 = R_6 + R_7 + R_8 + R_9 + R_{15} + R_{20} + R_{23} + R_{25} + 2R_{28} + R_{30} + R_{32} - R_{54} + R_{58} + R_{79} + R_{81} \\ - R_{83} + R_{90} + R_{91} + R_{101} + R_{110} + R_{121} + R_{122} + R_{125} + R_{131} + R_{132} + R_{134} + R_{135} + R_{141} \\ + R_{144} + R_{145} + R_{161} + 2R_{171} + R_{173} + 2R_{176} + 2R_{177} + R_{190} + R_{191} + R_{192} + R_{193} \\ + R_{194} + R_{195} + R_{196} + R_{197} + R_{198} + R_{199} + R_{201} - R_{208} + R_{217} + R_{222} + R_{224} + R_{225} \\ + R_{226} + R_{227} + R_{228} + R_{229} - R_{242} - R_{243} + R_{245} + R_{248} + R_{257} + R_{259} + R_{260} + R_{263} \\ + R_{274}$$

$$w_6 = -R_{171} + R_{182} + R_{190} + R_{191} + R_{192} + R_{193} + R_{194} + R_{195} + R_{197} - R_{200} - R_{202} - R_{203} + R_{217} \\ + R_{222} + R_{224} + R_{226} + R_{227} + R_{235} + R_{236} - R_{242} - R_{243} - R_{244} - R_{246} - R_{247} - R_{250} - R_{253} \\ - R_{255} - R_{256} - R_{262} - R_{264} - R_{266} - R_{267} - R_{269} - R_{271} + R_{273} - R_{275} - R_{276}$$

$$w_7 = -R_{181} - R_{182} - R_{183} - R_{184} - R_{185} + R_{199} + R_{228}$$

Steady-state relations (truncations in square brackets):

NNH:	$0 = -R_{204} - R_{205} - R_{206} - R_{207} - R_{208} - R_{209} - R_{210} - R_{211}$
HNO:	$0 = R_{192} + R_{194} + R_{197} + R_{201} + R_{212} - R_{213} - R_{214} - R_{215} - R_{216} + R_{263}$
NH:	$0 = -R_{190} - R_{191} - R_{192} - R_{193} - R_{194} - R_{195} - R_{196} - R_{197} - R_{198} - R_{199} + R_{200} + R_{202} + R_{203} + R_{208} \\ + R_{223} + R_{232} + R_{242} + R_{243} + R_{262} + R_{269}$
NH ₂ :	$0 = -R_{200} - R_{201} - R_{202} - R_{203} + R_{236} + R_{265} + R_{268} + R_{272} + R_{277} + R_{278} + R_{279}$
NH ₃ :	$0 = -R_{277} - R_{278} - R_{279}$
NO ₂ :	$0 = R_{186} + R_{187} - R_{188} - R_{189}$
HCN:	$0 = R_{219} + R_{221} - R_{230} - R_{231} - R_{232} - R_{233} - R_{234} - R_{235} - R_{236} - R_{237} + R_{240} + R_{242} + R_{243} + R_{246} \\ + R_{250} + R_{253} + R_{255} + R_{258} + R_{271} + R_{276}$
HNCO:	$0 = R_{235} + R_{249} + R_{252} - R_{262} - R_{263} - R_{264} - R_{265} - R_{266} - R_{267} - R_{268} - R_{269} + R_{270} + R_{273}$
H ₂ CN:	$0 = [R_{237}] - R_{238} + R_{256} + R_{275}$
HOCN:	$0 = R_{234} - R_{273}$
HCNO:	$0 = R_{251} + R_{254} - R_{270} - R_{271} - R_{272} + R_{274}$
HCNN:	$0 = R_{241} - R_{257} - R_{258} - R_{259} - R_{260} - R_{261}$
NCO:	$0 = R_{218} + R_{220} - R_{222} - R_{223} - R_{224} - R_{225} - R_{226} - R_{227} - R_{228} - R_{229} + R_{231} + R_{247} + R_{264} + R_{266} \\ + R_{267}$
CN:	$0 = -R_{217} - R_{218} - R_{219} - R_{220} - R_{221} + R_{230} + R_{233} + R_{239} + R_{244}$
N:	$0 = -R_{178} - R_{179} - R_{180} + R_{191} + R_{193} - R_{196} + R_{217} - R_{225} + R_{227} - R_{238} + R_{239} + R_{240} + R_{245} + R_{248} \\ - R_{275} - R_{276}$
C:	$0 = R_{49} - R_{90} - R_{122} - R_{123} - R_{124} - R_{239} - R_{244} - R_{245}$
CH ₂ O:	$0 = R_{10} - R_{15} + R_{16} + R_{17} + R_{26} - R_{32} + R_{54} - R_{56} - R_{57} - R_{58} + R_{60} + R_{65} + R_{83} + R_{92} + R_{94} - R_{101} \\ + R_{102} + R_{103} + R_{117} - R_{121} + R_{127} - R_{133} + R_{153} + R_{156} - R_{161} + R_{169} + R_{170} + R_{173}$
CH ₂ OH:	$0 = -R_{16} + R_{18} + R_{56} - R_{59} - R_{60} - R_{61} - R_{62} + R_{64} + R_{68} - R_{102} + R_{104} + R_{162} - R_{169}$
CH ₂ CO:	$0 = R_{24} - R_{29} - R_{30} - R_{80} - R_{81} + R_{82} + R_{107} - R_{114} + R_{133} + R_{140}$
CH ₃ OH:	$0 = -R_{18} - R_{19} + R_{59} + R_{63} - R_{68} - R_{69} + R_{95} - R_{104} - R_{105} + R_{147} - R_{162} - R_{163}$
HCCO:	$0 = R_{21} - R_{28} + R_{29} - R_{79} + R_{80} + R_{106} + R_{114} + R_{131} - R_{134} - R_{141} - R_{176} - 2R_{177} - R_{274}$
HCCOH:	$0 = -R_{82} + R_{108}$
CH ₃ O:	$0 = -R_{17} + R_{19} + R_{57} - R_{63} - R_{64} - R_{65} - R_{66} - R_{67} + R_{69} - R_{103} + R_{105} + R_{119} + R_{155} + R_{163} - R_{170}$
HCO:	$0 = R_7 + R_9 - R_{13} - R_{14} + R_{15} + R_{25} + R_{32} - R_{54} - R_{55} + R_{58} + R_{91} - R_{100} + R_{101} + R_{121} + R_{125} \\ + R_{132} + R_{135} - R_{160} + R_{161} - R_{166} - R_{167} - R_{168} + R_{171} + R_{173} + R_{248} + R_{259} + R_{260}$
CH:	$0 = -R_6 + R_{20} - R_{49} + R_{51} - R_{91} + R_{93} - R_{125} - R_{126} - R_{127} - R_{128} - R_{129} - R_{130} - R_{131} - R_{132} \\ - R_{133} - R_{134} - R_{240} - R_{241} - R_{246} - R_{247} - R_{248}$
CH ₂ :	$0 = -R_7 + R_{23} + R_{30} - R_{50} - R_{92} - R_{93} + R_{96} - R_{117} - R_{123} + R_{126} - R_{128} - R_{135} - R_{136} - 2R_{137} \\ - R_{138} - R_{139} - R_{140} - R_{141} + R_{142} + R_{143} + R_{148} + R_{151} + R_{152} + R_{238} - R_{242} - R_{249} - R_{250} - R_{251} \\ + R_{261}$
CH ₂ (s):	$0 = -R_8 - R_9 - R_{51} + R_{62} + R_{67} + R_{79} - R_{94} + R_{97} - R_{142} - R_{143} - R_{144} - R_{145} - R_{146} - R_{147} - R_{148} \\ - R_{149} - R_{150} - R_{151} - R_{152} - R_{153} - R_{154} - R_{243} - R_{252} - R_{253} - R_{254}$
CH ₃ :	$0 = -R_{10} + R_{11} + R_{25} + R_{26} + R_{50} - R_{52} + R_{53} + R_{61} + R_{66} + R_{81} - R_{95} - R_{96} - R_{97} + R_{98} + R_{110} \\ - R_{118} - R_{119} - R_{124} - R_{129} + R_{136} - R_{138} + 2R_{139} + R_{146} - R_{149} + 2R_{150} + R_{154} - R_{155} - R_{156} \\ - R_{157} - 2R_{158} - 2R_{159} - R_{160} - R_{161} - R_{162} - R_{163} - R_{164} - R_{165} - R_{211} - R_{255} - R_{256} - R_{275} \\ - R_{276}$

$$\begin{aligned}
\text{C}_2\text{H:} & 0 = -R_{20} + R_{22} - R_{70} - R_{106} + R_{109} + R_{123} - R_{171} - R_{172} \\
\text{C}_2\text{H}_2: & 0 = -R_{21} - R_{22} - R_{23} + R_{70} - R_{71} + R_{73} - R_{107} - R_{108} - R_{109} - R_{110} + R_{111} + R_{124} + R_{128} + R_{134} \\
& \quad + R_{137} + R_{172} + R_{174} + R_{177} \\
\text{C}_2\text{H}_3: & 0 = -R_{24} + R_{71} - R_{72} - R_{73} + R_{75} - R_{111} + R_{112} + R_{129} + R_{141} + R_{164} - R_{173} \\
\text{C}_2\text{H}_4: & 0 = -R_{25} + R_{72} - R_{74} - R_{75} + R_{77} - R_{112} + R_{130} + R_{138} + R_{149} - R_{164} - R_{174} + R_{175} \\
\text{C}_2\text{H}_5: & 0 = -R_{26} + R_{27} + R_{74} - R_{76} - R_{77} + R_{78} + R_{113} + R_{154} + R_{159} + R_{165} - R_{175} \\
\text{C}_2\text{H}_6: & 0 = -R_{27} + R_{76} - R_{78} - R_{113} - R_{154} + R_{158} - R_{165} \\
\text{O:} & 0 = -2R_1 - R_2 - R_3 - R_4 - R_5 - R_6 - R_7 - R_8 - R_9 - R_{10} - R_{11} - R_{12} - R_{13} - R_{14} - R_{15} - R_{16} - R_{17} \\
& \quad - R_{18} - R_{19} - R_{20} - R_{21} - R_{22} - R_{23} - R_{24} - R_{25} - R_{26} - R_{27} - R_{28} - R_{29} - R_{30} + R_{31} + R_{38} + R_{44} \\
& \quad + R_{86} + R_{122} + R_{125} + R_{155} + R_{178} + R_{179} - R_{181} - R_{182} + R_{185} - R_{187} - R_{188} - R_{190} + R_{194} - R_{200} \\
& \quad - R_{201} - R_{207} - R_{208} - R_{213} - R_{217} + R_{220} - R_{222} - R_{231} - R_{232} - R_{233} + R_{244} + R_{246} - R_{257} - R_{258} \\
& \quad + R_{259} - R_{262} - R_{263} - R_{264} - R_{279} \\
\text{HO}_2: & 0 = -R_4 + R_5 + R_{32} + R_{33} + R_{34} + R_{35} + R_{36} + R_{37} - R_{44} - R_{45} - R_{46} + R_{47} - R_{87} + R_{88} + R_{89} - 2R_{115} \\
& \quad - 2R_{116} - R_{117} - R_{118} - R_{119} - R_{120} - R_{121} + R_{157} + R_{168} + R_{169} + R_{170} + R_{175} + R_{184} - R_{186} \\
& \quad + R_{206} + R_{216} \\
\text{H}_2\text{O}_2: & 0 = -R_5 - R_{47} - R_{48} + R_{85} - R_{88} - R_{89} + R_{115} + R_{116} + R_{121} - R_{157}
\end{aligned}$$

APPENDIX II: THE VECTORS \mathbf{Y} , \mathbf{B}^S ($S = 38-44$), AND \mathbf{B}^C ($C = 45-49$)

$$\mathbf{y} = \begin{bmatrix} y_{\text{H}_2} & y_{\text{H}} & y_{\text{O}} & y_{\text{O}_2} & y_{\text{OH}} & y_{\text{H}_2\text{O}} \\ y_{\text{HO}_2} & y_{\text{H}_2\text{O}_2} & y_{\text{C}} & y_{\text{CH}} & y_{\text{CH}_2} \\ y_{\text{CH}_2(\text{S})} & y_{\text{CH}_3} & y_{\text{CH}_4} & y_{\text{CO}} & y_{\text{CO}_2} \\ y_{\text{HCO}} & y_{\text{CH}_2\text{O}} & y_{\text{CH}_2\text{OH}} & y_{\text{CH}_3\text{O}} \\ y_{\text{CH}_3\text{OH}} & y_{\text{C}_2\text{H}} & y_{\text{C}_2\text{H}_2} & y_{\text{C}_2\text{H}_3} \\ y_{\text{C}_2\text{H}_4} & y_{\text{C}_2\text{H}_5} & y_{\text{C}_2\text{H}_6} & y_{\text{HCCO}} \\ y_{\text{CH}_2\text{CO}} & y_{\text{HCCOH}} & y_{\text{N}} & y_{\text{NH}} & y_{\text{NH}_2} \\ y_{\text{NH}_3} & y_{\text{NNH}} & y_{\text{NO}} & y_{\text{NO}_2} & y_{\text{N}_2\text{O}} \\ y_{\text{HNO}} & y_{\text{CN}} & y_{\text{HCN}} & y_{\text{H}_2\text{CN}} & y_{\text{HCNN}} \\ y_{\text{HCNO}} & y_{\text{HOCN}} & y & \text{HNCO} & y_{\text{NCO}} \\ y_{\text{AR}} & y_{\text{N}_2} \end{bmatrix}^T$$

$$\mathbf{b}^i = \hat{\mathbf{b}}^i \mathbf{W}^{-1} \quad \mathbf{W}$$

$$= \begin{bmatrix} W_{\text{H}_2} & 0 & \cdot & \cdot & 0 \\ 0 & W_{\text{H}} & & & \cdot \\ \cdot & & \cdot & & \cdot \\ \cdot & & & \cdot & \cdot \\ 0 & \cdot & \cdot & \cdot & W_{\text{N}_2} \end{bmatrix}$$

$$\begin{aligned}
\hat{\mathbf{b}}^{38} = 0.25[& 0 \quad 2 \quad 3 \quad 0 \quad -1 \quad -2 \quad 2 \\ & -2 \quad 6 \quad 4 \quad 2 \quad 2 \quad 1 \quad 0 \quad 2 \quad 0 \quad 4 \quad 2 \\ & 4 \quad 4 \quad 0 \quad -1 \quad -2 \quad 0 \quad -2 \quad 0 \quad 2 \quad -1 \\ & 4 \quad -5 \quad 3 \quad 2 \quad 0 \quad -1 \quad 2 \quad 0 \quad -3 \quad 0 \\ & -2 \quad 2 \quad 1 \quad 3 \quad 4 \quad 0 \quad -2 \quad 0 \quad 2 \quad 0 \quad 0]
\end{aligned}$$

$$\begin{aligned}
\hat{\mathbf{b}}^{39} = 0.25[& 2 \quad 1 \quad -1 \quad 0 \quad 2 \quad 4 \quad 1 \quad 4 \\ & -6 \quad -5 \quad -4 \quad -4 \quad -2 \quad 0 \\ & -2 \quad 0 \quad -1 \quad 4 \quad -3 \quad -3 \quad 0 \\ & -10 \quad -8 \quad -7 \quad -6 \quad -5 \quad -4 \\ & -10 \quad -10 \quad -7 \quad -1 \quad -3 \\ & -2 \quad 0 \quad 1 \quad 0 \quad 1 \quad 0 \quad 1 \quad -6]
\end{aligned}$$

$$\begin{bmatrix} -4 & -3 & -5 & -5 & -3 \\ -5 & -6 & 0 & 0 \end{bmatrix}$$

$$\hat{\mathbf{b}}^{40} = 0.25 \begin{bmatrix} 0 & 0 & -1 & 0 & 1 & 0 & 0 & 2 \\ 2 & 2 & 2 & 2 & 1 & 0 & 0 & 0 \\ 0 & 0 & 0 & 2 & 3 & 2 & 2 & 2 \\ 2 & 1 & 2 & 3 & -1 & 2 & 2 & 1 \\ 0 & 0 & 1 & 0 & 0 & 4 & 3 & 3 \\ 2 & 4 & 2 & 2 & 0 & 0 \end{bmatrix}$$

$$\begin{aligned}
\hat{\mathbf{b}}^{41} = 0.25[& 2 \quad 1 \quad 0 \quad 0 \quad 1 \quad 2 \quad 1 \quad 2 \\ & -4 \quad -3 \quad -2 \quad -2 \quad -1 \quad 0 \\ & -4 \quad 0 \quad -3 \quad -2 \quad -1 \quad -1 \\ & 0 \quad -7 \quad -6 \quad -5 \quad -4 \quad -3 \\ & -2 \quad -7 \quad -6 \quad -6 \quad 0 \quad 1 \quad 2 \\ & 3 \quad 1 \quad 0 \quad 0 \quad 0 \quad 1 \quad -4 \quad -3 \\ & -2 \quad -3 \quad -3 \quad -3 \quad -3 \quad -4 \\ & 0 \quad 0]
\end{aligned}$$

$$\begin{aligned}
\hat{\mathbf{b}}^{42} = 0.25[& 2 \quad 1 \quad 0 \quad 0 \quad 1 \quad 2 \quad 1 \quad 2 \\ & -4 \quad -3, -2, -2, -1 \quad 0 \quad 0 \quad 0 \\ & 1 \quad -2 \quad -1 \quad -1 \quad 0 \quad -7 \\ & -6 \quad -5 \quad -4 \quad -3 \quad -2 \quad -7 \\ & -6 \quad -6 \quad 0 \quad -3 \quad -2 \quad -1 \\ & 1 \quad 0 \quad 0 \quad 0 \quad 1 \quad -4 \quad -3 \\ & -2 \quad -3 \quad -3 \quad -3 \quad -3 \quad -4 \\ & 0 \quad 0]
\end{aligned}$$

$$\begin{aligned}
\hat{\mathbf{b}}^{43} = 0.5[& 0 \quad 0 \quad 0 \quad 0 \quad 0 \quad 0 \quad 0 \quad 0 \quad 0 \\ & 0 \quad 0 \quad 0 \quad 0 \quad 0 \quad 0 \quad 0 \quad 0 \quad 0 \\ & 0 \quad 0 \quad 0 \quad 0 \quad 0 \quad 0 \quad 0 \quad 0 \quad 0 \\ & 0 \quad 0 \quad 0 \quad 1 \quad -1 \quad 1 \quad 1 \quad 0 \quad 1 \\ & 1 \quad 0 \quad 1 \quad -1 \quad -1 \quad -1 \quad 0 \quad 1 \\ & -1 \quad 1 \quad -1 \quad 0 \quad 0]
\end{aligned}$$

$$\begin{aligned}
\hat{\mathbf{b}}^{44} = 0.5[& -2 \quad -1 \quad -2 \quad -4 \quad -3 \quad -4 \\ & -5 \quad -6 \quad 4 \quad 3 \quad 2 \quad 2 \quad 1 \quad 0]
\end{aligned}$$

